



ELSEVIER

Journal of Chromatography A, 919 (2001) 157–179

JOURNAL OF  
CHROMATOGRAPHY A

www.elsevier.com/locate/chroma

# Quantitative analysis and synthesis of the electrokinetic mass transport and adsorption mechanisms of a charged adsorbate in capillary electrochromatography systems employing charged adsorbent particles

B.A. Grimes, A.I. Liapis\*

*Department of Chemical Engineering and Biochemical Processing Institute, University of Missouri-Rolla, Rolla, MO 65409-1230, USA*

Received 6 December 2000; received in revised form 7 March 2001; accepted 19 March 2001

## Abstract

The dynamic mathematical model of Grimes and Liapis [J. Colloid Interf. Sci. 234 (2001) 223] for capillary electrochromatography (CEC) systems operated under frontal chromatography conditions is extended to accommodate conditions in CEC systems where a positively charged analyte is introduced into a packed capillary column by a pulse injection (analytical mode of operation) in order to determine quantitatively the electroosmotic velocity, electrostatic potential and concentration profiles of the charged species in the double layer and in the electroneutral core region of the fluid in the interstitial channels for bulk flow in the packed chromatographic column as the adsorbate adsorbs onto the negatively charged fixed sites on the surface of the non-porous particles packed in the chromatographic column. Furthermore, certain key parameters are identified for both the frontal and analytical operational modes that characterize the performance of CEC systems. The results obtained from model simulations for CEC systems employing the analytical mode of operation indicate that: (a) for a given mobile liquid phase, the charged particles should have the smallest diameter,  $d_p$ , possible that still provides conditions for a plug-flow electroosmotic velocity field in the interstitial channels for bulk flow and a large negative surface charge density,  $\delta_o$ , in order to prevent overloading conditions; (b) sharp, highly resolute adsorption zones can be obtained when the value of the parameter  $\gamma_{2,\min}$ , which represents the ratio of the electroosmotic velocity of the mobile liquid phase under unretained conditions to the electrophoretic velocity of the anions ( $0 > \gamma_{2,\min} > -1$ ), is very close to negative one, but the rate at which the solute band propagates through the column is slow; furthermore, as the solute band propagates across larger axial lengths, the desorption zone becomes more dispersed relative to the adsorption zone especially when the value of the parameter  $\gamma_{2,\max}$ , which represents the ratio of the electroosmotic velocity of the mobile liquid phase under retained conditions to the electrophoretic velocity of the anions ( $0 > \gamma_{2,\max} > -1$ ), is significantly greater than  $\gamma_{2,\min}$ ; (c) when the value of the equilibrium adsorption constant,  $K_{A,3}$ , is low, very sharp, highly resolved adsorption and desorption zones of the solute band can be obtained as well as fast rates of propagation of the solute band through the column; (d) sharp adsorption zones and fast propagation of the solute band can be obtained if the value of the mobility,  $\nu_3$ , of the analyte is high and the value of the ratio  $\nu_1/\nu_3$ , where  $\nu_1$  represents the mobility of the cation, is low; however, if the magnitude of the mobility,  $\nu_3$ , of the analyte is small, dispersed desorption zones are obtained with slower rates of propagation of the solute band through the column; (e) good separation of analyte molecules having similar mobilities and different adsorption affinities can be obtained in short operational times with a very small column length,  $L$ , and the resolution can be increased by providing values of  $\gamma_{2,\min}$  and  $\gamma_{2,\max}$  that are very close to negative one; and (f) the

\*Corresponding author. Tel.: +1-573-341-4416; fax: +1-573-341-4377.

change in the magnitude of the axial current density,  $i_x$ , across the solute band could serve as a measurement for the rate of propagation of the solute band. © 2001 Elsevier Science B.V. All rights reserved.

**Keywords:** Electroosmotic flow; Electrophoretic migration; Electrochromatography; Adsorption; Charged adsorbate; Charged particles

---

## 1. Introduction

In capillary electrochromatography (CEC) systems a solute (analyte) could adsorb and desorb from a charged stationary phase packed in a column and is transported through the chromatographic column by: (i) electroosmotic flow (EOF) in the interstitial channels for bulk flow in the packed bed or monolith [1,2]; (ii) electrophoretic migration [2,3] if the solute is charged; (iii) axial dispersion [2,4,5] in the interstitial channels for bulk flow in the packed bed or monolith; (iv) film mass transfer in the interstitial channels for bulk flow in the packed bed or monolith [2,6]; (v) diffusion in the pores of the packed charged particles or monolith [7]; and (vi) intraparticle convection (flow) due to the EOF in the pores of the packed charged particles or monolith [7]. Furthermore, in CEC systems involving the adsorption and desorption of a charged analyte (adsorbate), the condition of electroneutrality [2] in the electroneutral core region of the fluid (in the interstitial channels for bulk flow and in the intraparticle pores) which is enveloped by the electrical double layer that exists near the liquid-solid interface, couples the transport of the adsorbate (analyte) to the transport of the background electrolyte species [2], and thus, the transport properties of the electrolyte species could influence significantly the resolution of the solute peak as well as the rate of propagation of the peak. A number of the mass transfer advantages offered by the CEC systems when compared to micro-HPLC systems, are due to the characteristics of the velocity field of the electroosmotic flow in CEC systems and have been presented in Refs. [1,2,4–7].

In order to evaluate and exploit properly the practical potential that CEC has shown to have and for it to become in a rational way a powerful separation method for the biotechnology and pharmaceutical industries, we would have to have a scientific understanding of the electrokinetic mass transport and adsorption and desorption mechanisms

involved in CEC systems, and to determine the quantitative effects of these mechanisms on the dynamic behavior of such systems. Grimes and Liapis [2] have constructed and solved numerically a mathematical model consisting of the momentum balance and Poisson equations [1,2] as well as the unsteady state continuity expressions for the cation and anion species of the background electrolyte and of a positively charged adsorbate (analyte) to provide the dynamic electroosmotic velocity, electrostatic potential, and concentration profiles in the electrical double layer and in the electroneutral core region of the interstitial channels for bulk flow as the positively charged adsorbate adsorbs onto the negatively charged fixed sites on the surface of charged non-porous spherical particles packed in a chromatographic column employing the frontal chromatography mode of operation. The results obtained from the model simulations of Grimes and Liapis [2] for CEC systems operated in the frontal chromatography mode, have provided significant physical insight and understanding with respect to the development and propagation of the dynamic profile of the concentration of the analyte and indicate that sharp, highly resolute adsorption fronts for a given column length can be obtained if: (i) the ratio of the electroosmotic velocity of the mobile liquid phase at the column entrance (after adsorption of the analyte has occurred) to the electrophoretic velocity of the anion is very close to negative one; (ii) the ratio of the mobility of the cation to the mobility of the analyte is not very large (less than two orders of magnitude), and this effect becomes more significant as the value of the equilibrium adsorption constant,  $K_{A,3}$ , of the analyte increases; and (iii) the concentration of the analyte relative to the concentration of the cation is increased.

In this work, the mathematical model of Grimes and Liapis [2] is extended to provide the dynamic electroosmotic velocity, electrostatic potential, and concentration profiles of the charged species in the

electrical double layer and in the electroneutral core region of the interstitial channels for bulk flow as a positively charged analyte (adsorbate) adsorbs onto the negatively charged fixed sites on the surface of charged non-porous spherical particles packed in a chromatographic column when the adsorbate (analyte) is introduced to the column by a pulse injection (analytical mode of operation).

## 2. Theoretical formulation

### 2.1. Mathematical model

In this work, the dynamic mathematical model of Grimes and Liapis [2] is employed to describe the unsteady state (dynamic) behavior of a positively charged adsorbate (analyte) which is introduced by a pulse injection to a capillary electrochromatography system employing a column packed with charged non-porous spherical adsorbent particles. Dilute solutions are considered in this work and the adsorption of the positively charged analyte onto the surface of the negatively charged non-porous particles is considered to occur infinitely fast (equilibrium adsorption occurs) and to be described by a linear isotherm of the form:

$$C_{3,S}(t, x) = K_{A,3} C_3(t, x, r = R_{ic}) \quad (1)$$

where  $C_{3,S}(t, x)$  represents the concentration of the positively charged analyte on the surface of the charged non-porous particles,  $K_{A,3}$  is the equilibrium adsorption constant of the adsorption mechanism, and  $C_3(t, x, r = R_{ic})$  denotes the concentration of the positively charged adsorbate in the layer of liquid adjacent to the surface of the charged non-porous particles. The variables  $t$ ,  $x$ , and  $r$  represent the time, the axial direction along the length of the column, and the radial direction along the radius,  $R_{ic}$ , of the interstitial channels for bulk flow in the packed bed, respectively. The expression for  $C_3(t, x, r = R_{ic})$  is given [2] by Eq. (2)

$$C_3(t, x, r = R_{ic}) = C_{3,ec}(t, x) \left[ \exp\left(-\frac{z_3 e \Phi(r = R_{ic})}{kT}\right) \right] \quad (2)$$

where  $C_{3,ec}(t, x)$  denotes the concentration of the

analyte in the electroneutral core region of the interstitial channels for bulk flow in the packed bed,  $z_3$  represents the charge number of the adsorbate,  $e$  is the charge of an electron,  $k$  represents the Boltzmann constant,  $T$  denotes the absolute temperature of the system, and  $\Phi(r = R_{ic})$  is the electrostatic potential at the surface of the interstitial channels which are formed from the surfaces of the packed charged non-porous particles. By employing Eq. (2) into Eq. (1), one obtains:

$$C_{3,S}(t, x) = \left[ K_{A,3} \left( \exp\left(-\frac{z_3 e \Phi(r = R_{ic})}{kT}\right) \right) \right] C_{3,ec}(t, x). \quad (3)$$

The surface charge density,  $\delta$  ( $\delta < 0$ ), will change as adsorption of the analyte occurs and the value of  $\delta$  at a time  $t$  and position  $x$  in the system will be given by the expression:

$$\delta = \delta_0 + \left( \frac{z_3 F}{\xi} \right) C_{3,S}(t, x) = \delta_0 + \left( \frac{z_3 F}{\xi} \right) \times \left[ K_{A,3} \left( \exp\left(-\frac{z_3 e \Phi(r = R_{ic})}{kT}\right) \right) \right] C_{3,ec}(t, x) \quad (4)$$

where  $\delta_0$  is the surface charge density at  $t=0$  (before any adsorption of analyte has occurred),  $F$  denotes the Faraday constant, and  $\xi$  is the column phase ratio ( $\xi = (1 - \varepsilon_b)(3/r_p) + (2/R)$ ) when both the surface of the column walls and the surface of the particles are charged [2], and  $\xi = (1 - \varepsilon_b)(3/r_p)$  when only the surface of the particles is charged;  $\varepsilon_b$  denotes the porosity of the packed bed,  $r_p$  is the radius of the particles, and  $R$  represents the radius of the chromatographic column). The electroneutrality condition in the electroneutral core region couples the material balance equations of the cations, anions, and of the analyte and is given by Eq. (5):

$$z_1 C_{1,ec}(t, x) + z_2 C_{2,ec}(t, x) + z_3 C_{3,ec}(t, x) = 0 \quad (5)$$

where  $z_1$  and  $z_2$  represent the charge numbers of the cation and anion of the electrolyte, respectively, and  $z_3$  denotes the charge number of the analyte, while  $C_{1,ec}(t, x)$ ,  $C_{2,ec}(t, x)$ , and  $C_{3,ec}(t, x)$  denote the concentrations of the cation, anion, and analyte species in the electroneutral core region, respectively. The

concentrations,  $C_i(t, x, r)$  (for  $i=1, 2, 3$ , where  $i=1$  denotes the cation of the electrolyte,  $i=2$  denotes the anion of the electrolyte, and  $i=3$  denotes the analyte), along the axial direction,  $x$ , and along the radius,  $r$ , of the interstitial channels for bulk flow at a given time  $t$  are obtained [2] from expression (6):

$$C_i(t, x, r) = C_{i,ec}(t, x) \left[ \exp\left(-\frac{z_i e \Phi(r)}{kT}\right) \right],$$

$$i = 1, 2, 3 \quad (6)$$

The dynamic profiles of: (i) the electroosmotic velocity,  $\langle v_x \rangle$ ; (ii) the electrostatic potential  $\Phi$ ; and (iii) the concentrations  $C_{i,ec}$  ( $i=1, 2, 3$ ) are obtained from the simultaneous solution of the momentum balance and Poisson equations, as well as of the continuity equations of species 1, 2, and 3 in the electroneutral core region of the interstitial channels for bulk flow, as presented in the model of Grimes and Liapis [2]. While Grimes and Liapis [2] studied the dynamic behavior of a positively charged analyte in CEC systems operated in the frontal chromatography mode, in this work the positively charged adsorbate is introduced to the capillary column by a pulse injection, and thus, the inlet concentration,  $C_{3,in}$ , of the analyte was taken to be described by the Gaussian form given by Eq. (7):

$$C_{3,in} = C_{3,max} \exp\left[-\frac{1}{2}\left(\frac{t - (t_{pd}/2)}{(t_{pd}/8)}\right)^2\right],$$

for  $t \geq 0$  (7)

where  $C_{3,max}$  denotes the maximum concentration of the analyte in the feed stream and  $t_{pd}$  represents the duration of the pulse injection.

## 2.2. Certain key parameters that characterize the dynamic behavior of CEC systems

In CEC systems involving a positively charged analyte and non-porous charged particles, the adsorption of the analyte onto the negatively charged surface of the stationary surface causes the magnitude of the charge on the surface to become less negative, and thus, the adsorption process induces a restructuring of the concentration distributions of the cations and anions of the background electrolyte as well as of the analyte along the radial direction,  $r$ , of

the interstitial channels for bulk flow at time  $t$  and axial position  $x$  in the column where analyte adsorbs. This restructuring during adsorption weakens the attractive electrostatic forces between the positively charged species (cations and adsorbate) in the liquid phase and the negatively charged stationary surface, and also weakens the repulsive electrostatic forces between the negatively charged species (anions) in the liquid phase and the negatively charged stationary phase. Therefore, the adsorption process requires positive charges to be expelled from the electrical double layer and enter the electroneutral core region of the interstitial channels, while negative charges are moving from the electroneutral core region into the electrical double layer. The anions of the background electrolyte are the only contributors of negative charge in the mobile liquid phase, and thus, the anions are required during the adsorption of the positively charged analyte to enter the electrical double layer and also balance the positive charges in the electroneutral core region of the interstitial channels for bulk flow. The restructuring of the concentration distributions of the charged species in the double layer that is due to the adsorption of the analyte, will change the space charge density [1,2] in the double layer while the concentration,  $C_{3,s}$ , of the analyte in the adsorbed phase will change the magnitude of the fixed charge density,  $\delta$  [2], on the wall of the interstitial channels for bulk flow. The changes in the magnitudes of the space charge density and  $\delta$  affect significantly the distribution of the electrostatic potential and through it the velocity field of the electroosmotic flow. Thus, the supply and removal of anions to and from the adsorption zone will significantly affect the performance of CEC systems. The cations, anions, and the analyte are transported to the adsorption front by a combination [2] of convective transport due to electroosmotic flow (EOF), electrophoretic transport, and diffusive transport. The convective electroosmotic velocity,  $\langle v_x \rangle$ , due to EOF is along the positive axial direction,  $x$ , of the column for all species, while the electrophoretic velocity,  $v_{elph,i}$  ( $v_{elph,i} = \nu_i z_i F E_x = D_i (z_i e E_x) / (kT)$ ) for  $i=1, 2, 3$ ;  $\nu_i$  is the mobility of species  $i$ ,  $D_i$  is the effective diffusion coefficient of component  $i$ , and  $E_x$  represents the applied electric potential difference per unit length along the axial direction,  $x$ , of the column) is along the positive axial direction,  $x$ ,

of the column for the cations and the positively charged analyte and along the negative axial direction,  $x$ , of the column for the anions. Thus, the ratio,  $\gamma_2$ , of the electroosmotic velocity,  $\langle v_x \rangle$ , of the mobile liquid phase to the electrophoretic velocity of the anion represents a useful parameter for characterizing the supply and removal of anions to and from the adsorption zone, and, of course, this ratio,  $\gamma_2$ , would always have a negative value. In CEC systems under the frontal [2] mode of operation, the parameter  $\gamma_{2,\min}$  represents the smallest value of  $\gamma_2$  and is defined as the ratio of the electroosmotic velocity,  $\langle v_x \rangle$ , of the mobile liquid phase at the downstream boundary of the adsorption zone (where there is no analyte present in the adsorbed phase ( $\delta = \delta_0$  in Eq. (4)) or in the liquid phase ( $C_{3,\text{ec}} = 0$ )) to the electrophoretic velocity of the anion, while the parameter  $\gamma_{2,\max}$  represents the largest value of  $\gamma_2$  and is defined as the ratio of the electroosmotic velocity,  $\langle v_x \rangle$ , of the mobile liquid phase at the upstream boundary of the adsorption zone (where maximum loading of the analyte in the adsorbed phase occurs) to the electrophoretic velocity of the anion. Since the electroosmotic velocity under retained (adsorption) conditions is always smaller than the electroosmotic velocity under unretained conditions [2], it is apparent that  $\gamma_{2,\min}$  will have the largest negative magnitude while  $\gamma_{2,\max}$  will have the smallest negative magnitude. For CEC systems where the positively charged analyte is introduced by pulse injection (analytical mode of operation),  $\gamma_{2,\min}$  is defined the same way as in CEC systems under the frontal mode of operation and  $\gamma_{2,\max}$  is defined as the ratio of the electroosmotic velocity evaluated at the maximum loading of the analyte in the adsorbed phase (maximum loading of the analyte occurs at the peak of the solute band and the value of  $\gamma_{2,\max}$  varies with time as the solute band spreads (or contracts) with time as it propagates through the column; in some systems the largest value of  $\gamma_{2,\max}$  could occur at time  $t = t_{\text{pd}}/2$  and position  $x = 0$  in the column where the value of  $C_{3,\text{in}}$  is equal to  $C_{3,\text{max}}$ , but in other systems the largest value of  $\gamma_{2,\max}$  could occur at some time  $t^* (t^* > t_{\text{pd}})$  and position  $x^* (x^* > 0)$  in the column) to the electrophoretic velocity of the anions. When the value of  $\gamma_{2,\min}$  or  $\gamma_{2,\max}$  is less than negative one, the magnitude of the electroosmotic velocity,  $\langle v_x \rangle$ , of the mobile liquid phase is larger than the magnitude of

the electrophoretic velocity of the anions, and when the value of  $\gamma_{2,\min}$  or  $\gamma_{2,\max}$  is greater than negative one then the magnitude of the electroosmotic velocity,  $\langle v_x \rangle$ , of the mobile liquid phase is smaller than the magnitude of the electrophoretic velocity of the anions. Therefore, three distinct combinations of  $\gamma_{2,\min}$  and  $\gamma_{2,\max}$  are possible in CEC systems involving a positively charged analyte and these combinations provide information regarding how the anions are supplied to or removed from the adsorption zone. These three combinations are as follows: in Case A,  $\gamma_{2,\min} > -1$  and  $\gamma_{2,\max} > -1$ ; in Case B,  $\gamma_{2,\min} < -1$  and  $\gamma_{2,\max} < -1$ ; and in Case C,  $\gamma_{2,\min} < -1$  and  $\gamma_{2,\max} > -1$ . In addition to  $\gamma_{2,\min}$  and  $\gamma_{2,\max}$ , it has been found [2] that the magnitude of the values of the equilibrium adsorption constant,  $K_{A,3}$ , the maximum value of the inlet concentration,  $C_{3,\text{in}}$ , of the analyte ( $C_{3,\text{in}} = C_{3,\text{max}}$ ), as well as the ratio,  $\nu_1/\nu_3$ , of the mobility of the cation to the mobility of the analyte affect significantly the dynamic behavior [2] of CEC systems. It should be noted here that it has been found [2] that the ratio,  $\nu_1/\nu_2$ , of the mobility of the cation to the mobility of the anion also affects the dynamic behavior of CEC systems, but the effect of the ratio  $\nu_1/\nu_2$  is not as significant as the effect of the parameters  $\gamma_{2,\min}$ ,  $\gamma_{2,\max}$ ,  $K_{A,3}$ ,  $C_{3,\text{max}}$ , and  $\nu_1/\nu_3$ .

### 2.3. Frontal CEC: Case A ( $\gamma_{2,\min} > -1$ and $\gamma_{2,\max} > -1$ )

In frontal CEC systems where  $\gamma_{2,\min} > -1$  and  $\gamma_{2,\max} > -1$ , the net molar flux of anions is along the negative [2] axial direction,  $x$ , of the column everywhere in the packed bed ( $0 \leq x \leq L$ , where  $L$  denotes the column length). Therefore, the anions enter the adsorption zone through the downstream boundary of the adsorption zone (the anions crash head on into the adsorption front) and the anions exit the adsorption zone from the upstream boundary of the adsorption zone. For given values of  $K_{A,3}$  and  $\nu_1/\nu_3$ , the results from model simulations [2] indicate that dispersed adsorption zones are obtained with fast rates of propagation of the adsorption front when the value of  $\gamma_{2,\max}$  approaches zero (if  $\gamma_{2,\max} = 0$ , overloading has occurred and there is no EOF and the system is no longer a CEC system), while when the value of  $\gamma_{2,\max}$  approaches negative one, very sharp (resolute) adsorption fronts are obtained with slow

rates of propagation of the adsorption front and, thus, it takes more time for the front to exit the column. The reason for these results is that for given values of  $K_{A,3}$  and  $\nu_1/\nu_3$  the anions must have a certain residence time within the adsorption zone in order to be present within the adsorption zone in an appropriate amount, so that the anions can distribute themselves through the adsorption zone in order to accommodate the restructuring of the concentrations of the species in the electrical double layer and maintain electroneutrality in the electroneutral core region of the interstitial channels. Thus, when the value of  $\gamma_{2,max}$  approaches zero the anions are moving very fast (due to electrophoretic transport) through the adsorption zone and, therefore, the thickness of the adsorption zone must be large (dispersed adsorption zone) in order to provide the appropriate residence time for the anions to move through the adsorption front, while when the value of  $\gamma_{2,max}$  approaches negative one the anions move very slowly through the adsorption zone and, therefore, only a very thin adsorption zone (resolute (sharp) adsorption zone) is required in order to provide the appropriate residence time for the anions to move through the adsorption zone.

For given values of  $\gamma_{2,min}$ ,  $\gamma_{2,max}$ , and  $K_{A,3}$ , values of the ratio  $\nu_1/\nu_3$  that are much greater than unity provide dispersed adsorption zones with fast rates of propagation of the adsorption front compared to systems with lower values of the parameter  $\nu_1/\nu_3$ . This occurs because the cations have a much stronger influence than the analyte on the rate that the adsorption zone propagates through the column and the cations spread the analyte downstream faster than the analyte can adsorb. When the value of  $\nu_1/\nu_3$  is close to unity, the adsorption zone is more resolute than it is for larger values of  $\nu_1/\nu_3$  because the cations no longer significantly compete with the analyte to determine the rate of propagation of the adsorption front; but, the time it takes for the adsorption zone to propagate through the column increases because the mobility,  $\nu_1$ , of the cation is smaller. When  $\nu_1/\nu_3 < 1$  even sharper adsorption fronts can be obtained because the cations hinder the ability of the analyte to move downstream, and consequently the adsorbate moves into the adsorbed phase more readily than it would propagate downstream; but, the rate of propagation of the adsorption

front is very slow since the cations hinder the propagation of the adsorption front as well as the fact that the analyte that arrives at the adsorption front has more of a tendency to move into the adsorbed phase rather than to propagate downstream. It should be noted that as the analyte becomes less concentrated relative [2] to the cations, the effect that large values of  $\nu_1/\nu_3$  ( $\nu_1/\nu_3 \gg 1$ ) have in spreading the adsorption zone increases because the cations contribute more of the positive charges to the system, while the effect that small values of  $\nu_1/\nu_3$  ( $\nu_1/\nu_3 \ll 1$ ) will have in sharpening the adsorption zone increases because again the cations contribute more of the positive charges to the system.

For given values of  $\gamma_{2,min}$ ,  $\gamma_{2,max}$ , and  $\nu_1/\nu_3$ , more resolute adsorption fronts can be obtained for lower values of  $K_{A,3}$  than those obtained when the value of  $K_{A,3}$  is large. When the value of  $K_{A,3}$  is small, the adsorption process expels only a small amount of positive charges from the electrical double layer and requires only a small amount of anions to enter into the electrical double layer, which implies that the adsorption process requires a shorter residence time for the anions to pass through the adsorption zone and, thus, the width of the adsorption zone (the degree of spreading of the adsorption front) will be small. For larger values of  $K_{A,3}$  more anions are required to enter into the electrical double layer in order to accommodate the adsorption process and this requires a longer residence time for the anions to pass through the adsorption zone, which implies that the adsorption zone will be more dispersed.

#### 2.4. Frontal CEC: Case B ( $\gamma_{2,min} < -1$ and $\gamma_{2,max} < -1$ )

In frontal CEC systems where  $\gamma_{2,min} < -1$  and  $\gamma_{2,max} < -1$ , the net molar flux of the anions is along the positive [2] axial direction,  $x$ , of the column everywhere in the packed bed ( $0 \leq x \leq L$ ). Therefore, the anions enter the adsorption zone through the upstream boundary of the adsorption zone and they exit the adsorption zone through the downstream boundary of the adsorption zone. When both  $\gamma_{2,min}$  and  $\gamma_{2,max}$  are close to negative one, very sharp resolute adsorption fronts could be obtained because the anions pass through the adsorption zone very slowly (the velocity of the EOF barely exceeds the

oppositely directed electrophoretic velocity of the anions and, thus, the anions propagate very slowly along the positive axial direction,  $x$ , of the column) and, therefore, the residence time required for the anions to pass through the adsorption zone (the residence time depends on the values of  $K_{A,3}$  and  $\nu_1/\nu_3$ ) can be realized when the adsorption zone is very thin (resolved adsorption front). As the velocity of the EOF increases relative to the electrophoretic velocity of the anions ( $\gamma_{2,\min}$  and  $\gamma_{2,\max}$  become much less than negative one), the adsorption front becomes more dispersed because the axial width of the adsorption zone must increase to provide the appropriate residence time for the anions to pass through the adsorption zone for the given values of  $K_{A,3}$  and  $\nu_1/\nu_3$ . It should be noted here that in Case B both the anions and the adsorption front propagate along the positive axial direction,  $x$ , of the column (in Case A, the anions propagate along the negative axial direction,  $x$ , of the column while the adsorption front propagates along the positive axial direction,  $x$ , of the column), and when  $\gamma_{2,\min}$  and  $\gamma_{2,\max}$  become much less than negative one in Case B the velocity of the anion species increases along positive  $x$  as well as the rate at which the adsorption front propagates through the column along positive  $x$ , and therefore, in Case B when the values of  $\gamma_{2,\min}$  and  $\gamma_{2,\max}$  become much less than negative one the relative speed between the anions and the adsorption front does not increase as significantly as the relative speed between the anions and the adsorption front in Case A when the values of  $\gamma_{2,\min}$  and  $\gamma_{2,\max}$  approach zero from negative one (as the values of  $\gamma_{2,\min}$  and  $\gamma_{2,\max}$  approach zero from negative one in Case A the velocity of the anions increases along negative  $x$  while the rate at which the adsorption front propagates along positive  $x$  increases) and, thus, the degree of spreading of the adsorption zone will be less marked in Case B than in Case A as the values of  $\gamma_{2,\min}$  and  $\gamma_{2,\max}$  diverge from negative one ( $\gamma_{2,\min}$  and  $\gamma_{2,\max}$  approach zero in Case A and  $\gamma_{2,\min}$  and  $\gamma_{2,\max}$  become much less than negative one in Case B) because the adsorption zone will not have to spread significantly in order to maintain the residence time required for the anions to pass through the adsorption zone for given values of  $K_{A,3}$  and  $\nu_1/\nu_3$ . However, since the anions enter the adsorption zone from the upstream boundary of the adsorption

zone where the magnitude of the electroosmotic velocity is lower than the electroosmotic velocity downstream of the adsorption zone, the concentration of the anions at the upstream boundary of the adsorption zone must be larger than the concentration of the anions at the downstream boundary of the adsorption zone, and as the adsorption front propagates through the column the concentration of the anions continuously decreases at the upstream boundary of the adsorption zone. If the length,  $L$ , of the packed bed is so long such that the concentration of the anions at the upstream boundary of the adsorption zone decreases to a value that cannot provide an appropriate molar flux of anions into the adsorption zone in order to facilitate the adsorption process before the mass wave exits the column, then the adsorption process will cease and the analyte will be leaked through the column.

For given values of  $\gamma_{2,\min}$ ,  $\gamma_{2,\max}$  and  $K_{A,3}$ , the effect of the ratio  $\nu_1/\nu_3$  on the resolution of the adsorption zone is similar to the effect that the ratio  $\nu_1/\nu_3$  had in Case A. However, since the sum,  $\Omega_2$ , of the electroosmotic and electrophoretic velocities of the anion is always less than the sum,  $\Omega_1$ , of the electroosmotic and electrophoretic velocities of the cations ( $\Omega_i = \langle v_x \rangle + \nu_i z_i F E_x$  for  $i = 1, 2, 3$ ), the cations must hinder the rate of propagation of the adsorption front in order to allow the anions to reach the adsorption zone and facilitate the adsorption process; in order for the cations to hinder the rate of propagation of the adsorption front the value of  $\nu_1/\nu_3$  must be less than unity.

The effect of the value of  $K_{A,3}$  on the resolution of the adsorption zone is similar to the effect that  $K_{A,3}$  had in Case A.

### 2.5. Frontal CEC: Case C ( $\gamma_{2,\min} < -1$ and $\gamma_{2,\max} > -1$ )

When the value of  $\gamma_{2,\min}$  is less than negative one, the anions would propagate through the column along the positive axial direction,  $x$ , in the region of the column downstream of the adsorption front. When the value of  $\gamma_{2,\max}$  is greater than negative one, the anions would propagate through the column along the negative axial direction,  $x$ , in the region of the column upstream of the adsorption front. Thus, the anions do not enter in this case the adsorption

zone and since the anions are required to provide an appropriate supply of negative charges within the adsorption zone in order to accommodate the restructuring of the concentrations of the charged species in the electrical double layer that must occur when the analyte adsorbs, the adsorption process might not occur and the analyte might be leaked through the column.

In the following section of this work results are presented for Case A ( $\gamma_{2,\min} > -1$  and  $\gamma_{2,\max} > -1$ ) when the CEC systems employ a positively charged analyte which is introduced to the capillary column by a pulse injection of the form given by Eq. (7). Results for Case B ( $\gamma_{2,\min} < -1$  and  $\gamma_{2,\max} < -1$ ) in CEC systems where the positively charged analyte is introduced by pulse injection will be presented in a future communication. Case C ( $\gamma_{2,\min} < -1$  and  $\gamma_{2,\max} > -1$ ) in CEC systems where the positively charged analyte is introduced by pulse injection will

not be studied because the adsorption process might not occur for the reasons discussed in the frontal CEC systems above, and thus, in CEC systems that satisfy Case C the analyte might not adsorb and could be leaked through the column.

### 3. Results and discussion

The theoretical results presented in Figs. 1–11 of this work were obtained from the numerical solution of the mathematical model presented by Grimes and Liapis in Ref. [2] when the value of the concentration of the analyte,  $C_{3,\text{in}}$ , in the column feed stream varies with time according to the functional form given by Eq. (7) of this work. The CEC system parameters and their values that remained unchanged in the simulations are the following: the radius,  $R$ , and the length,  $L$ , of the fused-silica capillary column

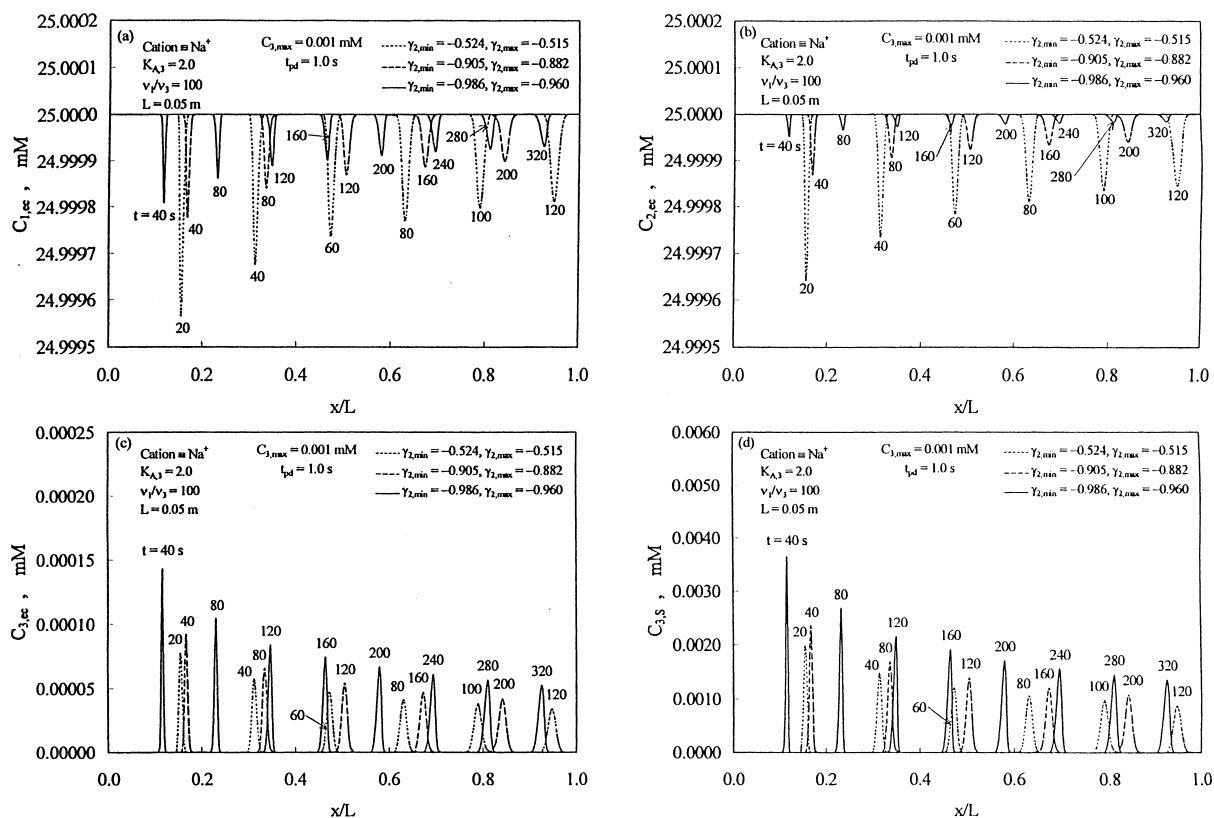


Fig. 1. Axial profiles of (a)  $C_{1,\text{ec}}$ , (b)  $C_{2,\text{ec}}$ , (c)  $C_{3,\text{ec}}$ , and (d)  $C_{3,\text{s}}$  at different times when  $t_{\text{pd}} = 1.0$  s.



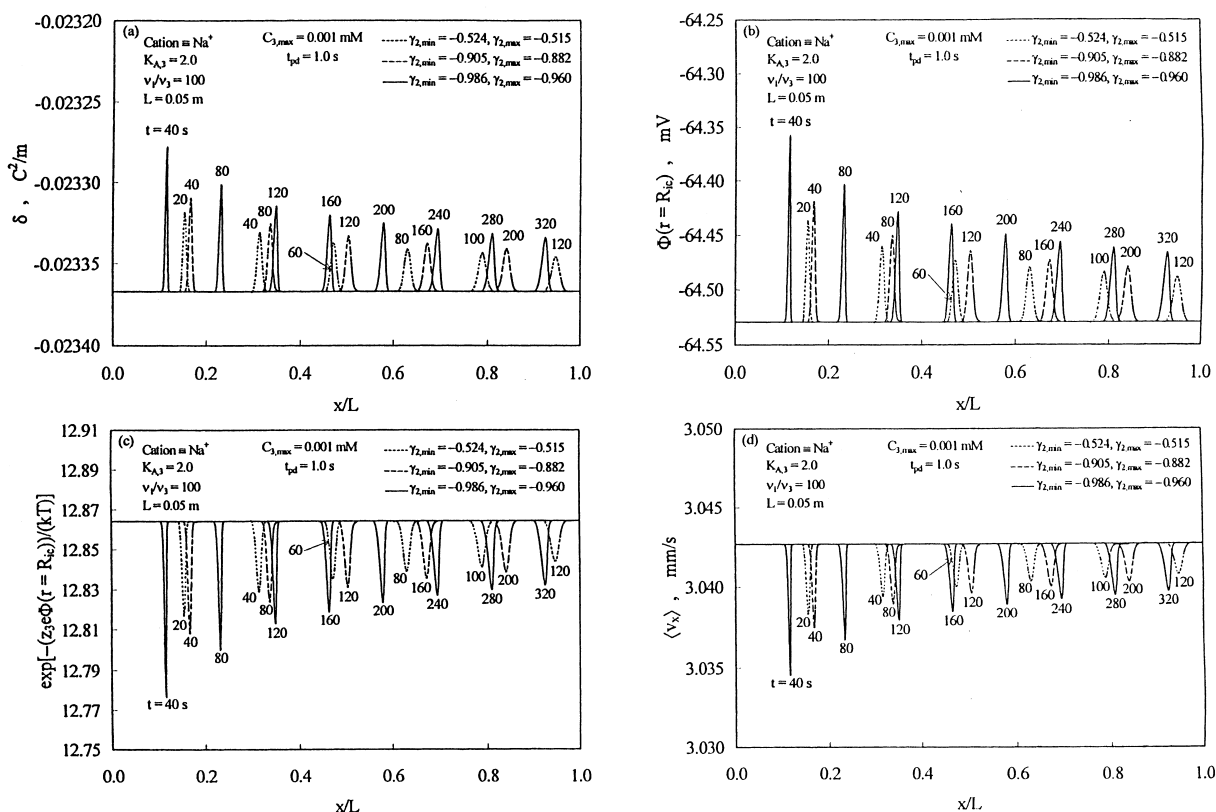


Fig. 2. Axial profiles of (a)  $\delta$ , (b)  $\Phi(r=R_{ic})$ , (c)  $\exp[-(z_s e \Phi(r=R_{ic})) / (kT)]$ , and (d)  $\langle v_x \rangle$  at different times when  $t_{pd} = 1.0$  s.

were 50  $\mu\text{m}$  and 0.05 m, respectively, the potential difference per unit length along the axis of the column,  $E_x$ , was 80 kV/m, the radius,  $r_p$ , of the charged non-porous silica particles was taken to be equal to 0.5  $\mu\text{m}$ , the temperature,  $T$ , was equal to 293.15 K, the mobile liquid phase is 80% acetonitrile–20% 25 mM (80:20, v/v) 1:1 electrolyte solution ( $z_+ = -z_- = 1$  and  $C_{+\infty} = C_{-\infty} = C_\infty = 25$  mM), the dielectric constant,  $\epsilon$ , of the mobile liquid phase is 47.8, the permittivity of free space,  $\epsilon_0$ , is  $8.85 \times 10^{-12} \text{ C}^2 / (\text{N} \cdot \text{m}^2)$ , the viscosity,  $\mu$ , of the mobile liquid phase is  $4.99 \times 10^{-4} \text{ kg} / (\text{m} \cdot \text{s})$ , the radius,  $R_{ic}$ , of the interstitial channels for bulk flow was taken to be [1,2] equal to 0.1667  $\mu\text{m}$ , the value of the surface charge density,  $\delta_0$ , is  $-0.02337 \text{ C} / \text{m}^2$ , the porosity,  $\epsilon_p$ , of the packed column is 0.35, the value of the column phase ratio,  $\xi$ , is  $3.94 \times 10^6 \text{ m}^{-1}$  [2], and the value of the conductivity factor,  $\chi$  ( $\chi$  is obtained from the ratio of the effective conductivity

of the packed capillary column filled with the electrolyte solution to the conductivity of the unpacked capillary column containing the same electrolyte solution [1,2]), was taken to be equal to 0.707 [1,2]. The values of the above parameters have been obtained from experimental [1] CEC systems and provide desirable in practice conditions for a plug-flow electroosmotic velocity field in the interstitial channels for bulk flow in the packed bed for the reasons given by Grimes and Liapis in Ref. [2]. In Figs. 1–4 of this work, the cation is  $\text{Na}^+$  and the anion is not specified because the value of the mobility,  $\nu_2$ , of the anion is varied; for the results of the simulations presented in Figs. 5–10 of this work, the electrolyte considered is NaCl and the values of the mobilities of the ions  $\text{Na}^+$  and  $\text{Cl}^-$  in the interstitial channels for bulk flow of the packed column are  $4.812 \times 10^{-13} \text{ (mol} \cdot \text{m)} / (\text{N} \cdot \text{s})$  and  $7.463 \times 10^{-13} \text{ (mol} \cdot \text{m)} / (\text{N} \cdot \text{s})$ , respectively.

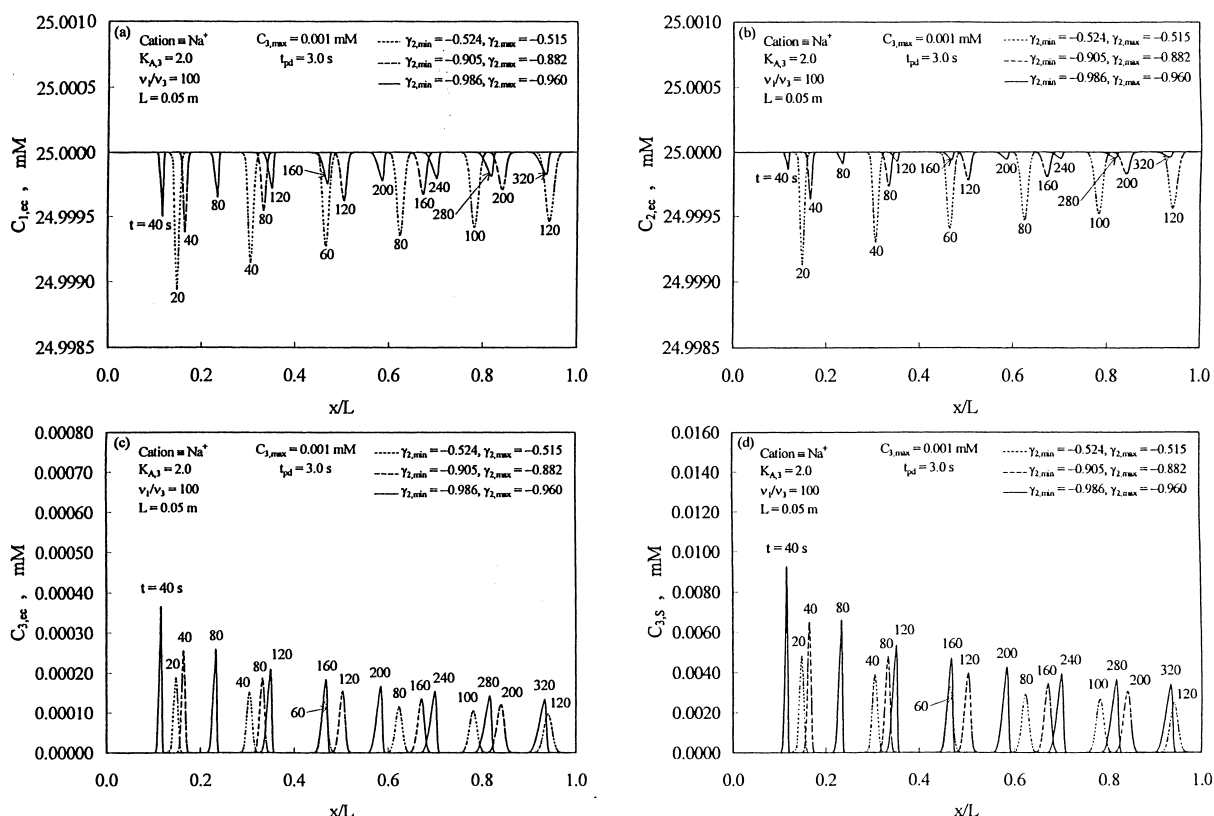


Fig. 3. Axial profiles of (a)  $C_{1,ec}$ , (b)  $C_{2,ec}$ , (c)  $C_{3,ec}$ , and (d)  $C_{3,S}$  at different times when  $t_{pd}=3.0$  s.

### 3.1. Effects of the parameters $\gamma_{2,min}$ and $\gamma_{2,max}$ on the dynamic behavior of analytical CEC systems

In Figs. 1–4 the axial profiles of  $C_{i,ec}$  ( $i=1, 2, 3$ ),  $C_{3,S}$ ,  $\delta$ ,  $\Phi(r=R_{ic})$ ,  $\exp[-(z_3 e \Phi(r=R_{ic})) / (kT)]$ , and  $\langle v_x \rangle$  are presented at different times for systems where  $C_{3,max}=0.001$  mM,  $K_{A,3}=2.0$ , and  $\nu_1/\nu_3=100$ ; the value of  $\nu_1$  is equal to the mobility of  $\text{Na}^+$  ( $\nu_1 = 4.812 \times 10^{-13}$  (mol·m)/(N·s)) and the anion is not specified because the value of  $\nu_2$  is varied to provide different values of  $v_{elph,2}$  in order to demonstrate the effect that the value of  $\gamma_{2,min}$  has on the speed (the rate at which the solute band propagates through the column) and resolution (the width of the solute band) of the solute band. The magnitude of the electroosmotic velocity,  $\langle v_x \rangle_{max}$ , in the regions of the column where there is no analyte present in the adsorbed and fluid phases is equal to 3.043 mm/s and the value of  $\gamma_{2,min}$  is equal to  $-0.524$ ,  $-0.905$

and  $-0.986$  when the value of  $\nu_2$  is equal to  $7.463 \times 10^{-13}$ ,  $4.356 \times 10^{-13}$  and  $4.000 \times 10^{-13}$  (mol·m)/(N·s), respectively. In Figs. 1 and 2 the duration time of the pulse injection,  $t_{pd}$ , is 1.0 s while in Figs. 3 and 4 the duration time of the pulse injection,  $t_{pd}$ , is 3.0 s. The results in Figs. 1c and 3c indicate that the solute band is highly resolved and propagates slowly through the column when the value of  $\gamma_{2,min}$  is close to negative one and that as  $\gamma_{2,min}$  increases, the solute band becomes more dispersed yet the rate at which the solute band propagates through the column increases. It is also worth noting that the concentration profile of the analyte in the solute band is significantly skewed downstream (the adsorption zone of the solute band is very sharp relative to the desorption zone of the solute band) when the value of  $\gamma_{2,min}$  is very close to negative one and that the concentration profile of the analyte is less skewed when the value of  $\gamma_{2,min}$  increases (becomes less

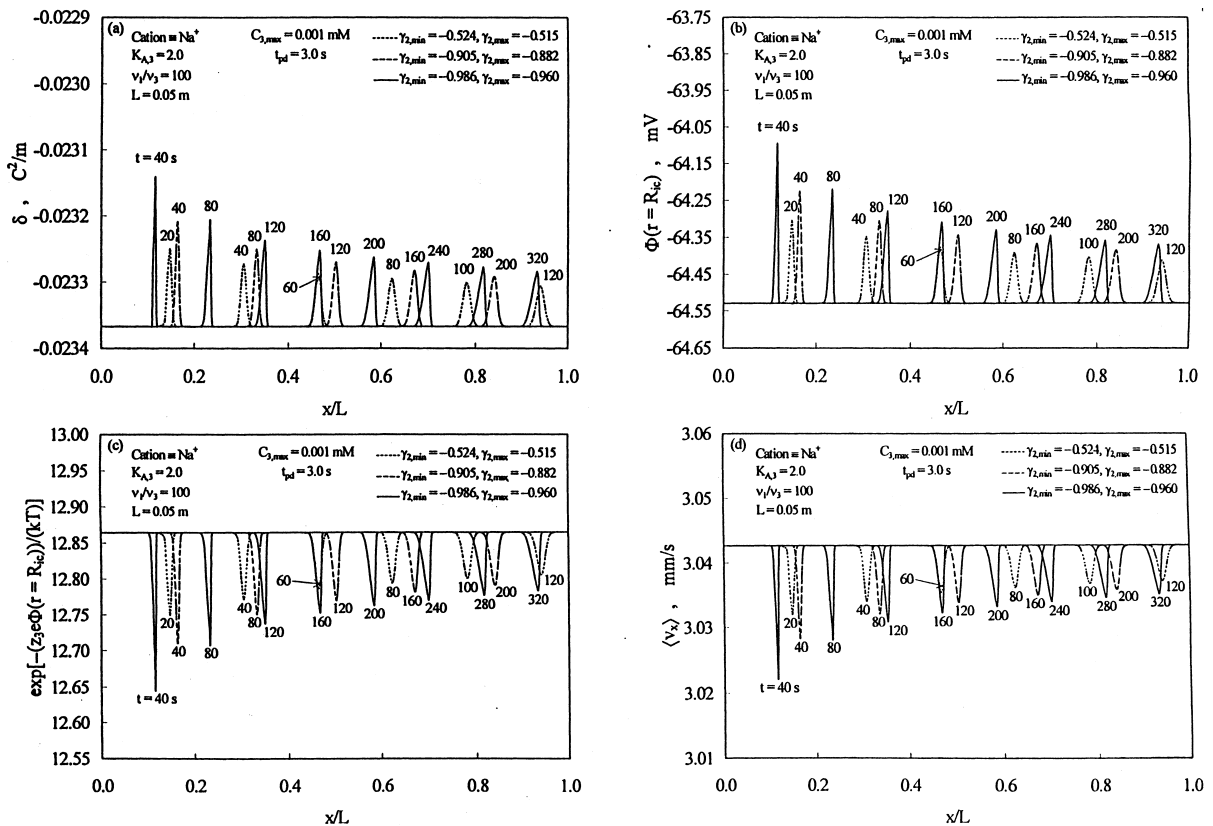


Fig. 4. Axial profiles of (a)  $\delta$ , (b)  $\Phi(r=R_{ic})$ , (c)  $\exp[-(z_3 e \Phi(r=R_{ic})) / (kT)]$ , and (d)  $\langle v_x \rangle$  at different times when  $t_{pd} = 3.0$  s.

negative). The reason that the solute band propagates slowly through the column and is very resolved with a skewed concentration profile of the analyte when the value of  $\gamma_{2,min}$  is very close to negative one, is because the anions that are required to enter the electrical double layer to facilitate the adsorption process are propagating very slowly in the negative  $x$  direction and, thus, in order for the anions to pass through the adsorption zone of the solute band with a certain residence time for adsorption to occur, the width of the adsorption zone should be very thin and the adsorption zone must propagate slowly through the column. The desorption zone of the solute band is more dispersed relative to the adsorption zone of the solute band (skewed concentration profile of the analyte), because the desorption process of the analyte in the desorption zone of the solute band is regulated by the supply of cations to the desorption zone (cations must enter the electrical double layer to

facilitate the desorption process since the value of  $\delta$  decreases (the value of  $\delta$  becomes more negative as the results in Figs. 2a and 4a indicate) when the analyte desorbs), and since the cations move faster through the desorption zone of the solute band relative to the speed at which the anions move through the adsorption zone of the solute band, the width of the desorption zone must be larger relative to the width of the adsorption zone of the solute band in order for the fast moving cations to pass through the desorption zone of the solute band with a certain residence time for desorption to occur. By comparing the results in Figs. 1c and 3c, it can be observed that the peak concentration of the adsorbate (analyte) within the solute band when  $t_{pd}$  is equal to 3.0 s is greater than the peak concentration of the adsorbate (analyte) within the solute band when  $t_{pd}$  is equal to 1.0 s because for the same value of C<sub>3,max</sub> the total mass of analyte injected into the column when  $t_{pd}$  is

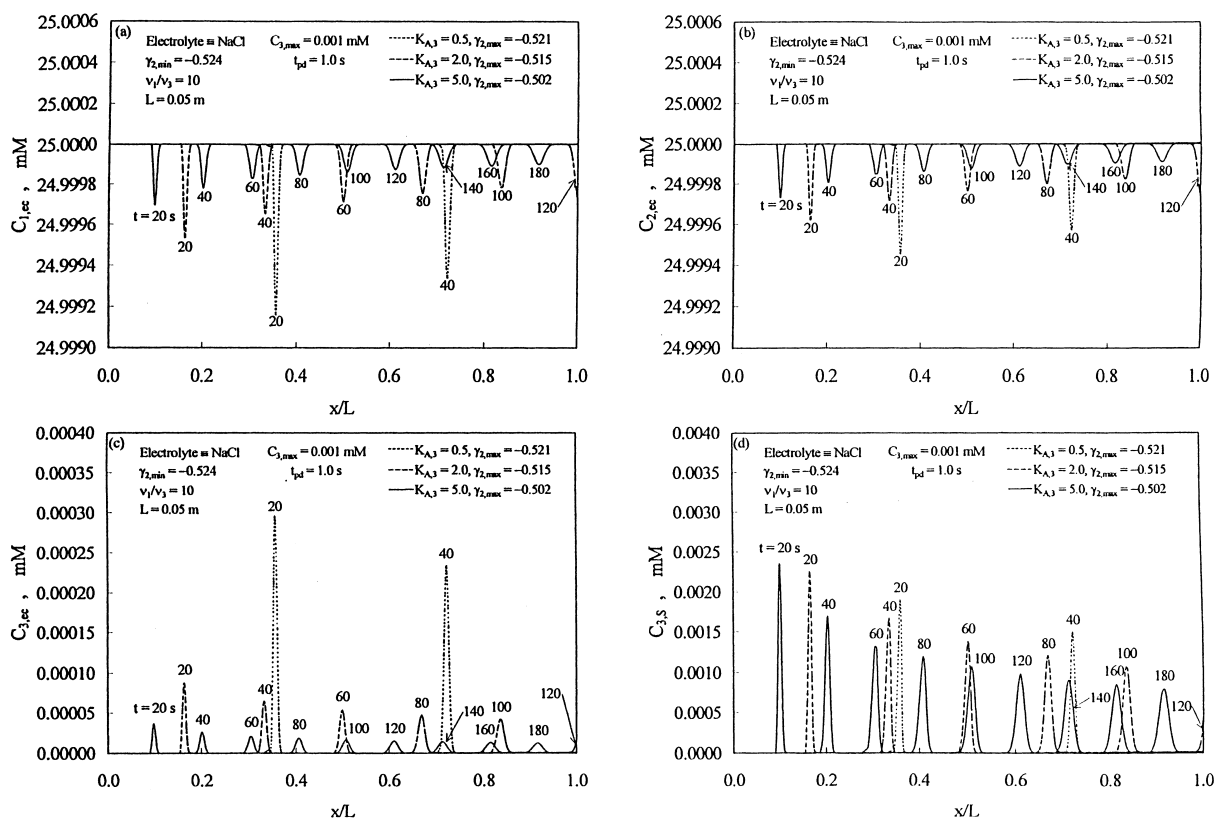


Fig. 5. Axial profiles of (a)  $C_{1,ec}$ , (b)  $C_{2,ec}$ , (c)  $C_{3,ec}$ , and (d)  $C_{3,s}$  at different times when  $t_{pd} = 1.0$  s.

equal to 3.0 s is greater than the total mass of analyte injected into the column when  $t_{pd}$  is equal to 1.0 s. However, the widths of the desorption and the adsorption zones of the solute band are strongly influenced by the mobilities of the cations and anions, respectively, and thus, the width of the solute band does not increase very much when the value of  $t_{pd}$  increases as the results in Figs. 1c and 3c indicate, and consequently, the peak concentration of the analyte in the solute band when  $t_{pd} = 3.0$  s must be greater than the peak concentration of the analyte in the solute band when  $t_{pd} = 1.0$  s. Furthermore, the results in Figs. 1 and 3 indicate that the rate at which the solute band propagates through the column is slightly slower when  $t_{pd} = 3.0$  s than when  $t_{pd} = 1.0$  s because the higher concentration of the analyte in the solute band increases the loading of the analyte and also the higher concentration of the analyte in the solute band requires more anions to enter the electri-

cal double layer in the adsorption zone and more cations to enter the electrical double layer in the desorption zone in order to facilitate the adsorption and desorption processes, and this results in slowing down the rate of propagation of the solute band. Figs. 1b and 3b indicate that the diffusive contribution to the net flux of anions in the desorption zone of the solute band is directed along positive  $x$  (the slope of the concentration profile of the anion,  $\partial C_{2,ec}/\partial x$ , in the desorption zone of the solute band is negative) and when the value of  $\gamma_{2,min}$  is very close to negative one, the electrophoretic velocity of the anion species barely exceeds the convective electroosmotic velocity of the anion species near the upstream boundary of the desorption zone (the anions are moving very slowly in the negative  $x$  direction), but since the anions are required to exit the solute band in order to balance the positive charges in the electroneutral core region upstream of

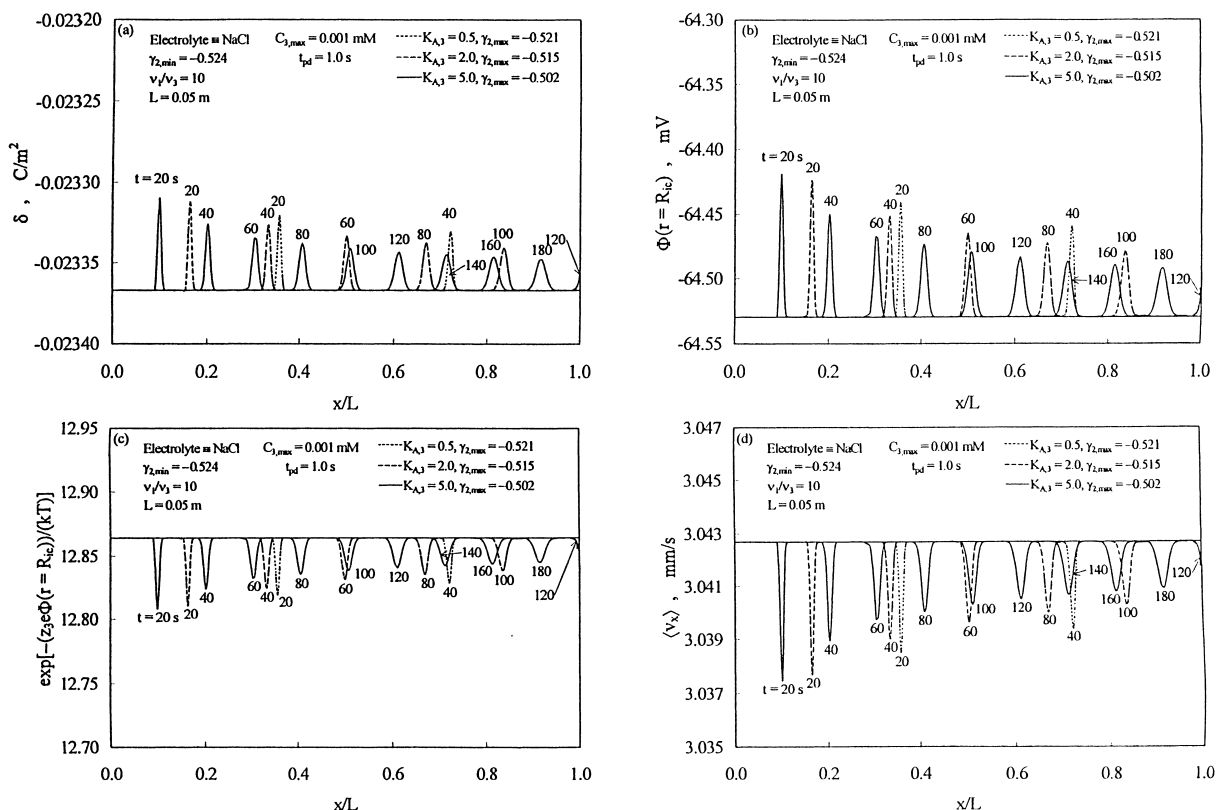


Fig. 6. Axial profiles of (a)  $\delta$ , (b)  $\Phi(r=R_{ic})$ , (c)  $\exp[-(z_3e\Phi(r=R_{ic}))/kT]$ , and (d)  $\langle v_x \rangle$  at different times when  $t_{pd} = 1.0$  s.

the solute band, the magnitude of the diffusive velocity of the anions along the positive  $x$  direction cannot be high enough to reverse the direction of the net flux of anions near the upstream boundary of the desorption zone. Therefore, it is worth noting here that by increasing significantly the value of  $C_{3,max}$  and/or the value of  $t_{pd}$  could act to substantially increase the dispersion of the desorption zone of the solute band when the value of  $\gamma_{2,min}$  is very close to negative one (especially when  $K_{A,3}$  is low,  $d_p$  is small, or  $\delta_0$  is very negative, because the electroosmotic velocity,  $\langle v_x \rangle$ , will not decrease as significantly in the solute band), because the value of  $\partial C_{2,ec}/\partial x$  must remain small in magnitude in order to keep the diffusive velocity directed along the positive axial direction,  $x$ , small within the desorption zone, which implies that when the peak concentration of the analyte is very large within the solute band due to large values of  $C_{3,max}$  and/or large values of  $t_{pd}$ , the width of the desorption zone

of the solute band may have to increase in order to keep the value of  $\partial C_{2,ec}/\partial x$  small in magnitude.

A very important consequence that results from the existence of the double layer in CEC systems employing negatively charged adsorbent particles to adsorb a positively charged analyte is that the concentration of the positively charged analyte increases very significantly along the positive  $r$  direction in the electrical double layer. Even at the peak of the solute band where the maximum loading (largest value of  $C_{3,s}$ ) of the analyte occurs (see Figs. 1d and 3d), the magnitude of the electrostatic potential at the wall of the interstitial channels for bulk flow does not increase by more than 0.5 mV for all the profiles of  $\Phi(r=R_{ic})$  presented in Figs. 2b and 4b, and thus, the magnitude of the exponential term in Eq. (3) varies at most between 12.777 and 12.864 for the results presented in Fig. 2c, and 12.645 and 12.864 for the results in Fig. 4c. Therefore, the concentration of the analyte in the fluid layer adja-

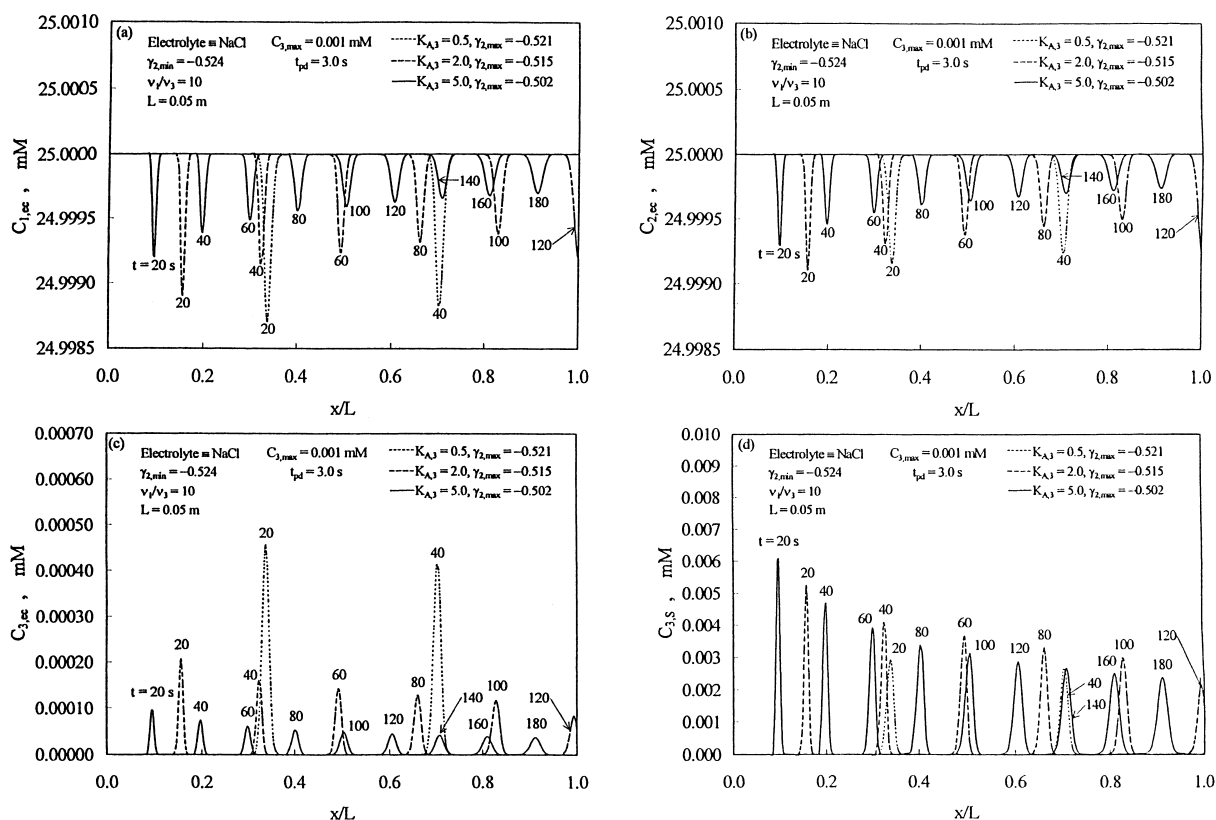


Fig. 7. Axial profiles of (a)  $C_{1,ec}$ , (b)  $C_{2,ec}$ , (c)  $C_{3,ec}$ , and (d)  $C_{3,s}$  at different times when  $t_{pd} = 3.0$  s.

cent to the surface of the negatively charged particles is more than an order of magnitude greater than the concentration of the analyte in the electroneutral core region of the interstitial channels for bulk flow, and therefore, the concentration of the analyte in the adsorbed phase can become much higher for a given value of  $K_{A,3}$ .

### 3.2. Effects of the parameter $\nu_1/\nu_3$ on the dynamic behavior of analytical CEC systems

In Figs. 5–8, the axial profiles of  $C_{i,ec}$  ( $i = 1, 2, 3$ ),  $C_{3,s}$ ,  $\delta$ ,  $\Phi(r = R_{ic})$ ,  $\exp[-(z_3 e \Phi(r = R_{ic})) / (kT)]$ , and  $\langle v_x \rangle$  are presented at different times for three different values of the equilibrium adsorption constant,  $K_{A,3}$ , when NaCl is the electrolyte,  $C_{3,max} = 0.001$  mM,  $\gamma_{2,min} = -0.524$ , and  $\nu_1/\nu_3 = 10$ . In Figs. 5 and 6 the duration time of the pulse injection,  $t_{pd}$ , is 1.0 s

while in Figs. 7 and 8 the duration time of the pulse injection,  $t_{pd}$ , is 3.0 s. By comparing the axial profiles of  $C_{3,ec}$  presented in Figs. 1c and 3c where  $\gamma_{2,min} = -0.524$ ,  $K_{A,3} = 2.0$ , and  $\nu_1/\nu_3 = 100$  to the axial profiles of  $C_{3,ec}$  presented in Figs. 5c and 7c where  $\gamma_{2,min} = -0.524$ ,  $K_{A,3} = 2.0$ , and  $\nu_1/\nu_3 = 10$ , one can observe in Figs. 5c and 7c, where the value of the ratio  $\nu_1/\nu_3$  is equal to 10, that the solute band propagates through the column at a slightly faster rate and is slightly less dispersed than the solute band in Figs. 1c and 3c where the value of the ratio  $\nu_1/\nu_3$  is equal to 100 (the value of the mobility,  $\nu_1$ , of the cation remains unchanged in Figs. 1–8 while the mobility,  $\nu_3$ , of the analyte in Figs. 5–8 is ten times larger than the mobility of the analyte in Figs. 1–4), and furthermore, in Figs. 3c and 7c where the analyte is more concentrated in the solute band due to the longer duration time,  $t_{pd}$ , of the pulse injection, the difference in the rate of propagation and

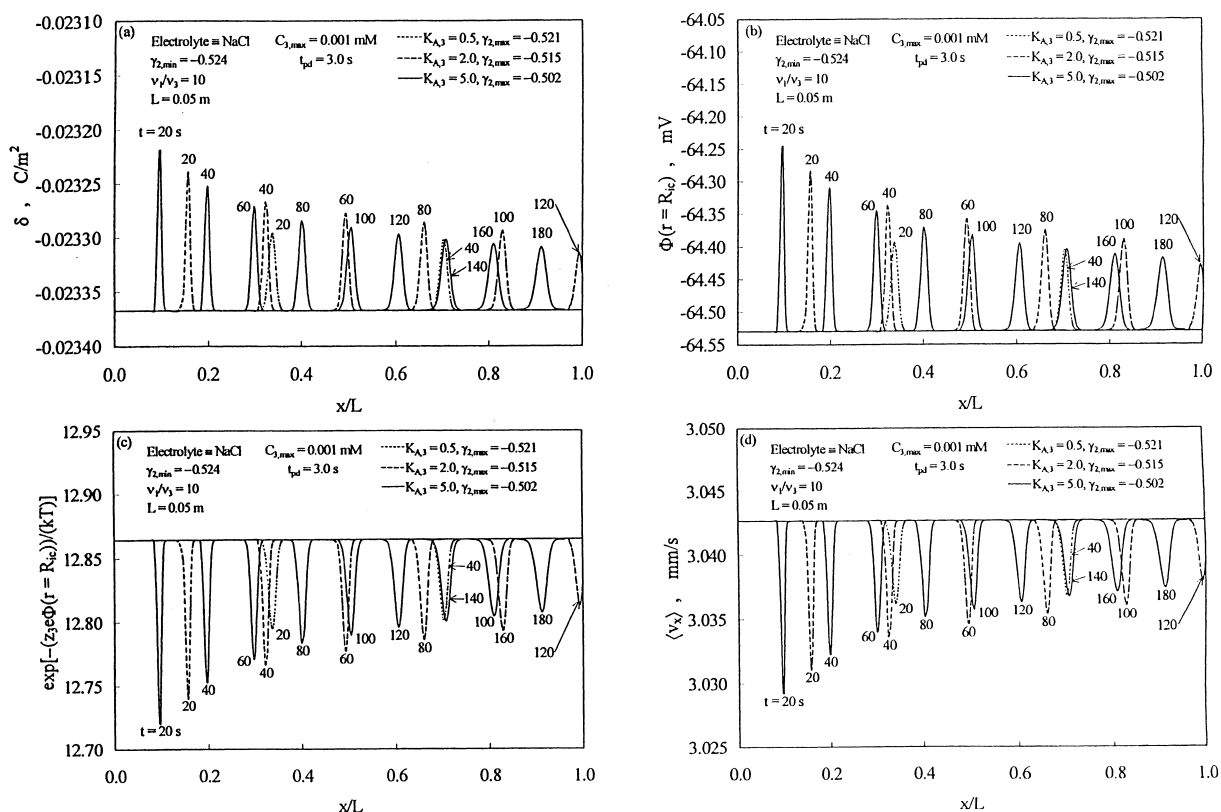


Fig. 8. Axial profiles of (a)  $\delta$ , (b)  $\Phi(r=R_{ic})$ , (c)  $\exp[-(z_{3e}\Phi(r=R_{ic}))/kT]$ , and (d)  $\langle v_x \rangle$  at different times when  $t_{pd} = 3.0$  s.

resolution of the solute band due to the different values of the ratio  $\nu_1/\nu_3$  is more significant. The effect of the value of the ratio  $\nu_1/\nu_3$  on the resolution of the adsorption zone of the solute band in the analytical CEC systems of Case A considered in this work, is similar to the effect of the value of the ratio  $\nu_1/\nu_3$  regarding the resolution of the adsorption zone in frontal CEC systems of Case A [2] discussed above. Since the mobility of the analyte,  $\nu_3$ , was increased relative to the mobility of the cation species,  $\nu_1$ , to provide a smaller value of the ratio  $\nu_1/\nu_3$ , the desorption zone of the solute band is less dispersed when the value of  $\nu_1/\nu_3$  is equal to 10 because the analyte molecules that desorb propagate downstream faster relative to the rate at which the desorbed analyte molecules propagate downstream when the value of  $\nu_3$  is smaller ( $\nu_1/\nu_3 = 100$ ), and consequently, the desorption zone of the solute band is not as dispersed when the value of the ratio  $\nu_1/\nu_3$  is equal to 10 compared to the system where the

value of the ratio  $\nu_1/\nu_3$  is equal to 100. However, since the concentration of the analyte relative to the concentration of the cations increases in the solute band when the value of  $t_{pd}$  is equal to 3.0 s compared to the system where the value of  $t_{pd}$  is equal to 1.0 s, the rate at which the solute band propagates through the column is slower when  $t_{pd}$  is equal to 3.0 s because (i) the slower analyte has more of an influence on the rate of propagation of the solute band due to its increased concentration relative to the faster cations; (ii) the larger concentration,  $C_{3,ec}$ , of the analyte in the electroneutral core region requires the concentration of the analyte in the fluid layer adjacent to the surface of the particles to increase which allows more analyte to be loaded onto the surface of the particles, and the increased loading of analyte imposes a greater demand for anions to be supplied to the electrical double layer in order to facilitate the adsorption process; and (iii) the increased loading of the analyte

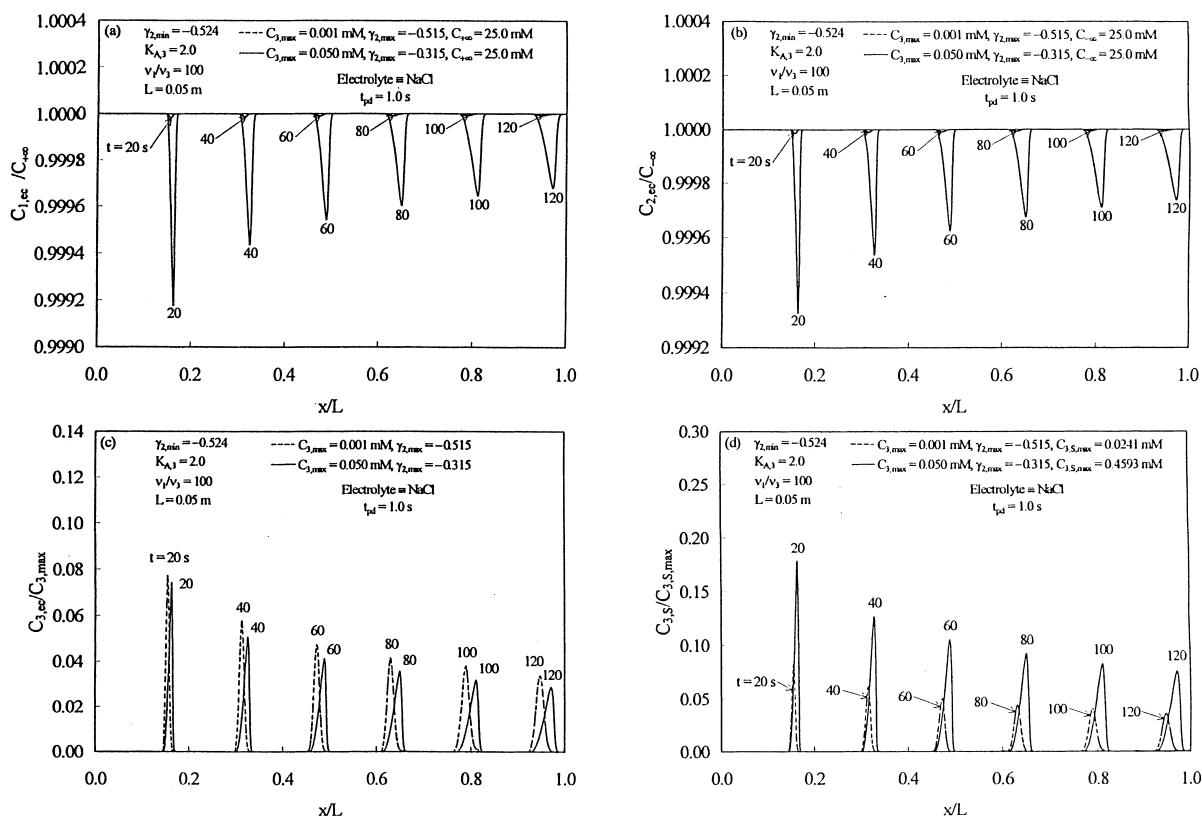


Fig. 9. Axial profiles of (a)  $C_{1,ec}/C_{+\infty}$ , (b)  $C_{2,ec}/C_{-\infty}$ , (c)  $C_{3,ec}/C_{3,max}$  and (d)  $C_{3,S}/(C_{3,S,max})$  at different times when  $t_{pd} = 1.0$  s.

imposes a greater demand for cations to be supplied to the electrical double layer in order to facilitate the desorption process; the processes in items (i)–(iii) act synergistically and their net effect is to slow down the rate of propagation of the solute band.

### 3.3. Effects of the parameter $K_{A,3}$ on the dynamic behavior of analytical CEC systems

The results in Figs. 5c and 7c indicate that very sharp (highly resolved) solute bands that propagate down the column in reasonably short times can be obtained when the value of  $K_{A,3}$  is low (that is, when the analyte does not have a very strong affinity to go into the adsorbed phase); when the value of  $K_{A,3}$  increases, the solute band is much more dispersed and propagates much more slowly through the column. The reason that more resolute adsorption fronts can be obtained for lower values of  $K_{A,3}$  than

those obtained when the values of  $K_{A,3}$  are large is because lower values of  $K_{A,3}$  require only a small amount of anions to enter into the electrical double layer, which implies that the adsorption process requires a shorter residence time for the anions to pass through the adsorption zone and, thus, the width of the adsorption zone will be small. For larger values of  $K_{A,3}$  more anions are required to enter into the electrical double layer in order to facilitate the adsorption process and this requires a longer residence time for the anions to pass through the adsorption zone, which implies that the adsorption zone will be more dispersed. Similarly, when the value of  $K_{A,3}$  is small, the desorption process expels only a small amount of anions from the electrical double layer and requires only a small amount of positive charges (mostly cations) to enter into the electrical double layer, which implies that the desorption process requires a shorter residence time for



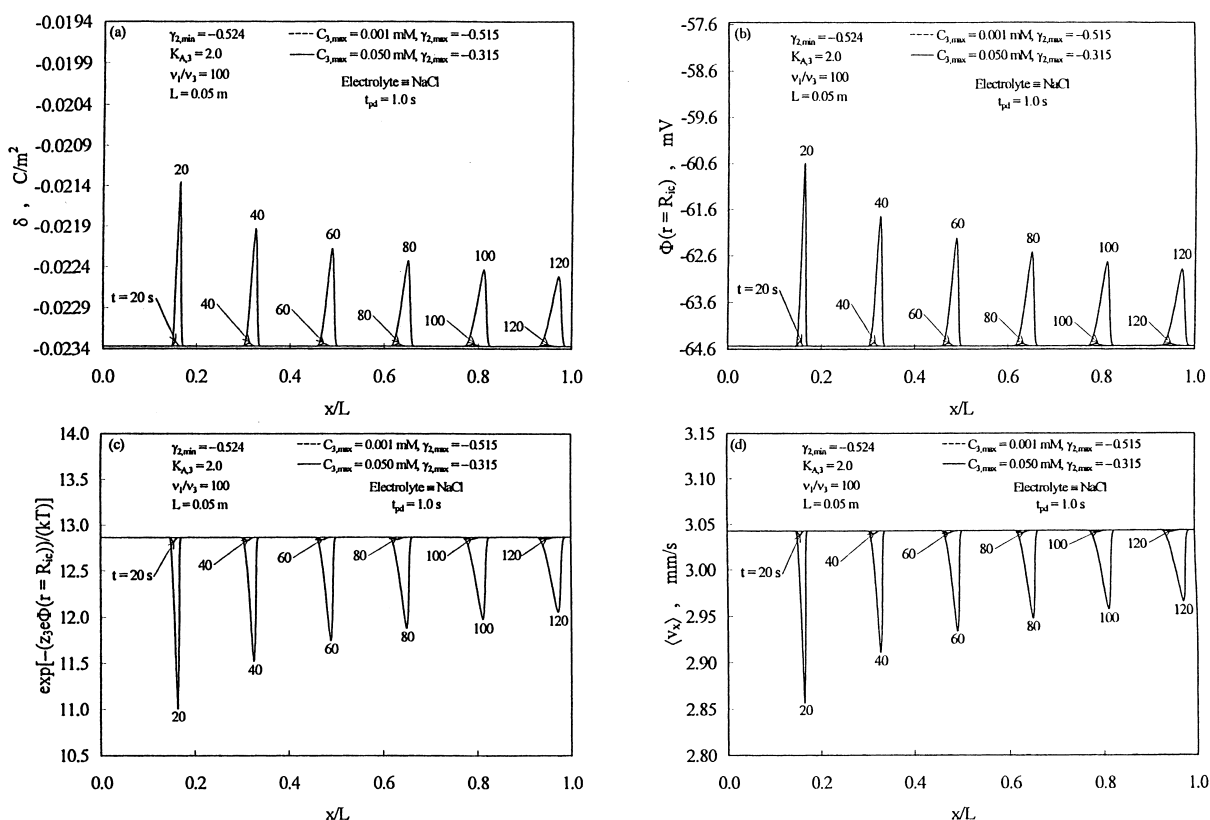


Fig. 10. Axial profiles of (a)  $\delta$ , (b)  $\Phi(r=R_{ic})$ , (c)  $\exp[-(z_3 e \Phi(r=R_{ic}))/kT]$ , and (d)  $\langle v_x \rangle$  at different times when  $t_{pd} = 1.0$  s.

the cations to pass through the desorption zone and, thus, the width of the desorption zone (the degree of spreading of the desorption zone of the solute band) will be small. For larger values of  $K_{A,3}$  more cations are required to enter into the electrical double layer in order to facilitate the desorption process and this requires a longer residence time for the cations to pass through the desorption zone, which implies that the desorption zone of the solute band will be more dispersed. In addition to the effect that the residence time of the cations in the desorption zone has on the resolution of the desorption zone, the desorption zone of the solute band is less dispersed when the value of  $K_{A,3}$  is low because simply the analyte has a lower affinity to be in the adsorbed phase and, thus, the analyte can desorb and move downstream much faster when the value of  $K_{A,3}$  is small as opposed to when the value of  $K_{A,3}$  is large. The solute band propagates faster through the column when the value

of  $K_{A,3}$  is low because (i) the analyte molecules have relatively more of a tendency to propagate downstream than to adsorb; (ii) there is less of a demand for the anions to enter the double layer to facilitate the adsorption process; and (iii) there is less of a demand for the cations to enter the double layer to facilitate the desorption process. The results in Figs. 6a and 8a show that the magnitude of the local surface charge density,  $\delta$ , increases (becomes less negative) within the solute band due to the loading of the positively charged analyte onto the negatively charged surface of the particles and, thus, the magnitude of the electrostatic potential,  $\Phi(r=R_{ic})$ , at the wall of the interstitial channels for bulk flow increases (see Figs. 6b and 8b) within the solute band while the magnitude of the electroosmotic velocity,  $\langle v_x \rangle$ , decreases (see Figs. 6d and 8d) within the solute band. It is worth noting here that the increased concentration of the analyte in the electrical double

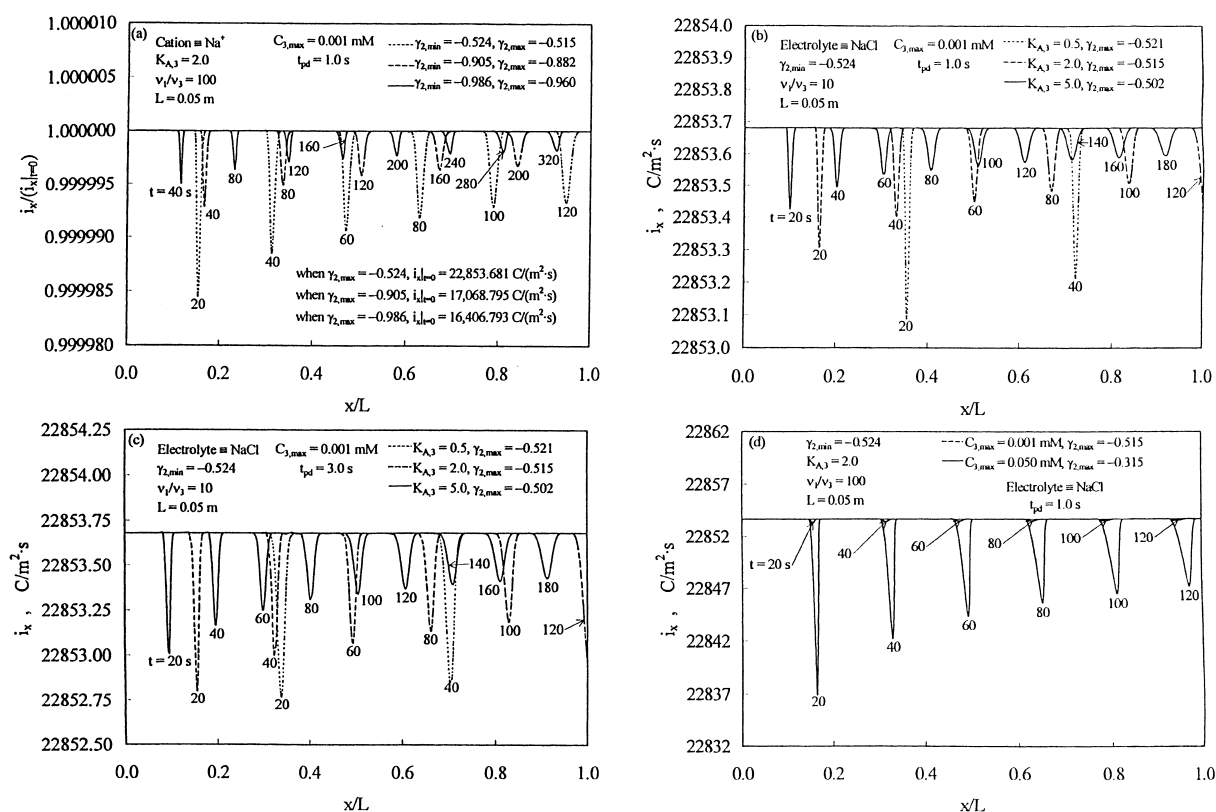


Fig. 11. Axial profiles of  $i_x/(i_x|_{t=0})$  and  $i_x$  at different times when  $t_{pd} = 1.0$  s and  $t_{pd} = 3.0$  s.

layer that is due to the magnitude of the electrostatic potential,  $\Phi$ , in the electrical double layer along with the value of  $K_{A,3}$  (see Eq. (3) above and also note the magnitude of the exponential terms presented in Figs. 6c and 8c), has a very significant impact on the way the analyte distributes itself between the adsorbed and fluid phases. If one examines the results presented in Figs. 5d and 7d, it can be observed that, at a given time, when the value of  $K_{A,3}$  is equal to 0.5 the concentration of the analyte in the adsorbed phase is not significantly smaller than the concentration of the analyte in the adsorbed phase when the value of  $K_{A,3}$  is equal to 5.0, and this is because the analyte is more concentrated relative to the cations in the electroneutral core region of the interstitial channels when  $K_{A,3}$  is equal to 0.5 as opposed to when  $K_{A,3}$  is equal to 5.0 (see Fig. 5a and c and Fig. 7a and c) and, thus, the analyte will contribute more of the positive charge to the space charge density of the electrical double layer which leads to a very high

concentration of the analyte in the fluid layer adjacent to the wall of the interstitial channels (the surface of the charged non-porous particles) when  $K_{A,3}$  is equal to 0.5 relative to the concentration of the analyte in the fluid layer adjacent to the wall of the interstitial channels when  $K_{A,3}$  is equal to 5.0, and the high concentration of the analyte at  $r = R_{ic}$  acts to increase the concentration,  $C_{3,s}$ , of the analyte in the adsorbed phase even when the value of  $K_{A,3}$  is small. By considering the previous statement and comparing the results in Fig. 5d to the results presented in Fig. 7d, one can observe that the effect of the longer duration time,  $t_{pd}$ , of the pulse injection in increasing the peak concentration of the analyte in the fluid phase of the solute band provides a larger difference between the concentrations of the analyte in the adsorbed phase for the various values of  $K_{A,3}$ , because for the larger value of  $t_{pd}$  the increased concentration of the analyte in the electroneutral core region of the solute band relative to the concentration

of the cations in the electroneutral core region of the solute band (compare Fig. 5a and c to Fig. 7a and c) requires the analyte to contribute more of the positive charges to the space charge density of the double layer, which increases the concentration of the analyte in the fluid layer adjacent to the surface of the charged particles and, thus, the amount of adsorbate that adsorbs increases for increasing values of  $K_{A,3}$ . Finally, the results in Figs. 5c and 7c indicate that the rate at which the solute band propagates through the column decreases when the value of  $t_{pd}$  increases for the same reasons discussed for the results presented in Figs. 1–4. If one compares the time it takes for each solute band in Figs. 5c and 7c to propagate 1.75 cm ( $x/L=0.35$ ), it can be observed that when  $K_{A,3}=0.5$  the solute band propagates 1.75 cm in less than 20 s, while when  $K_{A,3}=2.0$  the solute band propagates 1.75 cm in about 40 s, and when  $K_{A,3}=5.0$  the solute band takes more than 60 s to propagate 1.75 cm. The implication of this result is very significant because it shows that good separation of adsorbate molecules that have similar mobilities and very different affinities for adsorption onto the stationary phase could be achieved with columns that are less than 2.0 cm long, and furthermore, if one considers the sharpness of the solute bands and the very high concentrations of the analyte in the adsorbed phase at early times and short distances along the  $x$  direction of the column for the results presented in Figs. 1–4 where the value of  $\gamma_{2,\min}$  is close to negative one, it might be possible to provide conditions in CEC systems where one might obtain solute zones in the effluent stream that are more resolved than the solute zones that are injected into the column. These results indicate that in addition to the reasons discussed in Ref. [1], CEC systems are ideal for miniaturization because good separation and resolution can be achieved with a considerably short axial column length,  $L$ , as well.

### 3.4. Effects of the parameter $C_{3,\max}$ on the dynamic behavior of analytical CEC systems

In Figs. 9–10 the axial profiles of  $C_{1,ec}/C_{+\infty}$ ,  $C_{2,ec}/C_{-\infty}$ ,  $C_{3,ec}/C_{3,\max}$ ,  $C_{3,S}/C_{3,S,\max}$ ,  $\delta$ ,  $\Phi(r=R_{ic})$ ,  $\exp[-(z_3 e \Phi(r=R_{ic}))/kT]$ , and  $\langle v_x \rangle$  are presented at

different times for systems where  $C_{3,\max}=0.001$  mM and  $C_{3,\max}=0.050$  mM. In Figs. 9–10,  $\gamma_{2,\min}=-0.524$ ,  $t_{pd}=1.0$  s,  $K_{A,3}=2.0$ , and  $\nu_1/\nu_3=100$  for both values of  $C_{3,\max}$  considered. Furthermore, in Fig. 9,  $C_{3,S,\max}$  is defined as the concentration of the analyte in the adsorbed phase when the concentration of the analyte in the electroneutral core region of the interstitial channels is equal to  $C_{3,\max}$ , and  $C_{+\infty}$  and  $C_{-\infty}$  represent, respectively, the concentrations of the cations and anions in the electroneutral core region of the interstitial channels at time  $t=0$  when there is no analyte present in the column. The results in Fig. 9c indicate that when the value of  $C_{3,\max}$  increases, the rate that the downstream boundary (front) of the solute band propagates through the column increases while the position of the upstream boundary of the adsorption zone at any given time is almost the same for both values of  $C_{3,\max}$  presented in Fig. 9c; the solute band is slightly more dispersed, and the concentration profile of the analyte in the solute band is skewed downstream. The reason that when  $C_{3,\max}$  is equal to 0.050 mM the adsorption zone of the solute band is very sharp compared to the adsorption zone of the solute band when  $C_{3,\max}$  is equal to 0.001 mM is due to the combination of (i) the increased loading of the analyte that arises from the larger values of  $C_{3,ec}$  within the solute band that causes the analyte molecules in the adsorption zone to have relatively more of a tendency to go into the adsorbed phase as opposed to propagating downstream; and (ii) the increased concentration of the analyte,  $C_{3,ec}$ , relative to the cations,  $C_{1,ec}$ , within the solute band weakens the influence that the highly mobile cations ( $\nu_1/\nu_3=100$ ) have to spread the slower analyte downstream (when  $C_{3,\max}=0.001$  mM, the highly mobile cations are very concentrated relative to the slower analyte in the solute band and, thus, they have a strong influence to spread the analyte downstream which broadens the adsorption zone). Furthermore, the desorption zone of the solute band is sharper when  $C_{3,\max}=0.001$  mM compared to when  $C_{3,\max}=0.050$  mM, because the low concentration of the analyte relative to the cations in the solute band strengthens the influence of the highly mobile cations to spread the desorbed analyte downstream into the adsorption zone of the solute band. In effect, the results in Figs. 9 and 10 indicate how the influence of the parameter  $\nu_1/\nu_3$  on the resolution of the solute

band is conditioned on the concentration of the cations,  $C_{1,ec}$ , relative to the concentration of the analyte,  $C_{3,ec}$ , in the solute band. When  $C_{3,max}$  is equal to 0.050 mM the front of the solute band propagates through the column faster than the front of the solute band when  $C_{3,max}$  is equal to 0.001 mM because when the value of  $C_{3,max} = 0.050$  mM, the analyte is much more concentrated relative to the cations in the electroneutral core region of the interstitial channels compared to when  $C_{3,max} = 0.001$  mM, as shown in Fig. 9a and c, and this implies that the analyte is significantly much more concentrated in the fluid layer adjacent to the surface of the particles, and therefore, more analyte is loaded onto the surface of the charged particles when the analyte is more concentrated in the fluid phase; but as Fig. 10a and b suggest, the adsorption process causes the magnitude of  $\delta$  and  $\Phi$  to increase (become less negative) very significantly through the adsorption zone when the analyte is more concentrated in the fluid phase which causes the magnitude of the exponential term to decrease significantly and this decrease in the magnitude of the exponential term acts quickly to deter the preponderance of the analyte to go into the adsorbed phase and forces the concentrated adsorption zone to move downstream.

### 3.5. Implications of the dynamic behavior of the axial current density, $i_x$ , for identification of the state of analytical CEC systems

The results in Fig. 11 show at different times the profile of (a) the dimensionless axial current density,  $i_x/(i_x|_{t=0})$ , in the packed column for the simulations presented in Figs. 1 and 2, where  $C_{3,max} = 0.001$  mM,  $\nu_1/\nu_3 = 100$ ,  $K_{A,3} = 2.0$ ,  $Na^+$  is the cation, and  $t_{pd} = 1.0$  s; the value of  $i_x|_{t=0}$  ( $i_x|_{t=0}$  denotes the value of the axial current density at time  $t=0$  when only the electrolyte species are present in the column) is equal to 22 853.681, 17 068.795 and 16 406.793 C/(m<sup>2</sup>·s) when the value of  $\gamma_{2,min}$  is  $-0.524$ ,  $-0.905$ , and  $-0.986$ , respectively; (b) the axial current density,  $i_x$ , in the packed column for the simulations presented in Figs. 5 and 6 where  $K_{A,3}$  is varied,  $t_{pd} = 1.0$  s,  $C_{3,in} = 0.001$  mM,  $\gamma_{2,min} = -0.524$ ,  $\nu_1/\nu_3 = 10$ , and NaCl is the electrolyte; (c) the axial current density,  $i_x$ , in the packed column for the simulations pre-

sented in Figs. 7 and 8 where  $K_{A,3}$  is varied,  $t_{pd} = 3.0$  s,  $C_{3,in} = 0.001$  mM, and NaCl is the electrolyte; and (d) the axial current density,  $i_x$ , in the packed column for the simulations presented in Figs. 9 and 10, where  $C_{3,max}$  is varied,  $t_{pd} = 1.0$  s,  $\gamma_{2,min} = -0.524$ ,  $\nu_1/\nu_3 = 100$ ,  $K_{A,3} = 2.0$ , and NaCl is the electrolyte. The value of  $i_x$  in Fig. 11 is obtained from Eq. (8):

$$i_x = \left[ -F \sum_{i=1}^3 z_i D_i \left( \frac{z_i e C_i(t, x, r)}{kT} (-E_x) + \frac{\partial C_i(t, x, r)}{\partial x} \right) \right] + \chi_1 v_x(r) F \sum_{i=1}^3 z_i C_i(t, x, r) \quad (8)$$

where  $\chi_1$  denotes the electric conductivity factor [2] which is obtained from the ratio of the effective conductivity of the capillary column to the conductivity of the unobstructed fluid; the value of  $\chi_1$  was taken to be equal to 0.707 [2]. The velocity term  $v_x(r)$  in Eq. (8) was determined from Eq. (45) of Ref. [2]. The results in Fig. 11 indicate that the value of  $i_x$  decreases within the solute band because the concentrations of the electrolyte species are lower in the solute band and the less mobile analyte molecules are present in the mobile liquid phase. Furthermore, the results in Fig. 11a–d also show that the location of the lowest value of the axial current density occurs at the location of the peak of the analyte concentration in the solute band and, thus, the magnitude of  $i_x$  and/or the change in the value of  $i_x$  across the solute band could serve as a measurement for the rate of propagation of the solute band through the column.

## 4. Conclusions

The dynamic mathematical model of Grimes and Liapis [2] for CEC systems operated under frontal chromatography conditions has been extended to accommodate conditions in CEC systems where a positively charged analyte is introduced into a packed capillary column by a pulse injection (analytical mode of operation) in order to determine quantitatively the electroosmotic velocity, electrostatic potential and concentration profiles of the charged species in the double layer and in the

electroneutral core region of the fluid in the interstitial channels for bulk flow in the packed chromatographic column as the adsorbate adsorbs onto the negatively charged fixed sites on the surface of the non-porous particles packed in the chromatographic column. Furthermore, through the structure of the dynamic mathematical model and through simulations performed with this model, certain key parameters have been identified for both the frontal and analytical operational modes that characterize the performance of CEC systems. In this work, results were presented for CEC systems satisfying the conditions of Case A.

The results obtained from model simulations for CEC systems employing the analytical mode of operation indicate that when conditions that provide a plug-flow electroosmotic velocity profile in the interstitial channels for bulk flow of the packed bed are employed, then sharp, highly resolved adsorption zones of a solute band can be obtained (for Case A) when the value of  $\gamma_{2,\min}$  is very close to negative one, while the desorption zone of the solute band is more dispersed relative to the adsorption zone (the concentration profile of the analyte is skewed downstream) when the value of  $\gamma_{2,\min}$  is close to negative one. The dispersion of the desorption zone relative to the dispersion of the adsorption zone increases significantly as the solute band propagates further downstream. If the maximum concentration of the analyte,  $C_{3,\max}$ , in the pulse injection is very large such that the value of  $\gamma_{2,\max}$  is significantly greater than  $\gamma_{2,\min}$ , the spreading of the desorption zone relative to the spreading of the adsorption zone might increase significantly, and therefore, it might be advantageous to employ dilute concentrations of the analyte in the pulse injection. In CEC systems where the values of  $\gamma_{2,\min}$  and  $\gamma_{2,\max}$  are very close to negative one (Case A), the overall spreading of the adsorption zone is slightly less marked than when the values of  $\gamma_{2,\min}$  and  $\gamma_{2,\max}$  are significantly greater than negative one; however, the rate at which the solute band propagates through the column is much slower in CEC systems where the values of  $\gamma_{2,\min}$  and  $\gamma_{2,\max}$  are close to negative one when compared to CEC systems where the values of  $\gamma_{2,\min}$  and  $\gamma_{2,\max}$  are significantly greater than negative one. The results from model simulations also suggest that

sharp, highly resolute adsorption and desorption zones of the solute band that propagate very fast through the column can be obtained when the value of the equilibrium adsorption constant,  $K_{A,3}$ , of the analyte is low; when the value of  $K_{A,3}$  increases, the adsorption and desorption zones of the solute band become more dispersed and the solute band propagates more slowly through the column. The results from model simulations suggest that when the value of the ratio,  $\nu_1/\nu_3$ , of the mobility of the cation to the mobility of the analyte is large and the concentration of the analyte is very small relative to the concentration of the cations, the cations can act to spread the adsorption zone of the solute band downstream causing the adsorption zone to become dispersed, and this effect is less significant when the concentration of the analyte increases relative to the concentration of the cations. The results from model simulations suggest that longer duration times of the pulse injection cause the concentration of the analyte at the peak of the solute band to increase significantly while the longer duration times of the pulse injection do not significantly affect the degree of spreading of the solute band. Furthermore, it has been observed that the solute band becomes more dispersed and the concentration profile of the analyte becomes skewed more significantly downstream as the value of  $C_{3,\max}$  increases. The results of this work also indicate that the rate of propagation of the solute band in CEC systems is very different for analyte molecules that have similar mobilities and different adsorption affinities, and the results also indicate that when  $\gamma_{2,\min}$  is very close to negative one (Case A) the solute band is very resolute at early times and short distances along the axial direction  $x$  of the column before the desorption zone of the solute band spreads significantly compared to the adsorption zone of the solute band, and therefore, it may be advantageous to employ a very short column length,  $L$ , for CEC systems operated in the pulse injection mode.

Finally, the dynamic behavior of the axial current density,  $i_x$ , profiles in CEC systems operated in the analytical mode indicates that the magnitude of  $i_x$  and/or the change in the value of  $i_x$  across the solute band could serve as a measurement for the rate of propagation of the solute band through the column.

## 5. Nomenclature

$C_i(t, x, r)$	concentration of component $i$ ( $i = 1, 2, 3$ ) in the column, mol/m <sup>3</sup>	$k$	Boltzmann constant, J/K
$C_{i,ec}$	concentration of component $i$ ( $i = 1, 2, 3$ ) in the electroneutral core region of the interstitial channels for bulk flow, mol/m <sup>3</sup>	$L$	length of the capillary column, m
$C_{3,in}$	concentration of the positively charged analyte in the feed stream of the column, mol/m <sup>3</sup>	$N_0$	Avogadro's number, mol <sup>-1</sup>
$C_{3,max}$	maximum concentration of the positively charged analyte in the feed stream of the column ( $C_{3,in} = C_{3,max}$ when $t = t_{pd}/2$ in Eq. (7)), mol/m <sup>3</sup>	$R$	radius of the fused-silica capillary column, m
$C_{3,S}$	concentration of the positively charged analyte on the surface of the charged adsorbent particles, mol/m <sup>3</sup>	$R_{ic}$	radius of the interstitial channels for bulk flow in the packed bed, m
$C_{3,S,max}$	concentration of the positively charged analyte in the adsorbed phase when the concentration of the analyte in the electroneutral core region of the interstitial channels is equal to $C_{3,max}$ for the given value of $\delta_0$ , mol/m <sup>3</sup>	$r$	radial coordinate of the interstitial channels, m
$C_{+\infty}$	concentration of the cations in the electroneutral core region of the interstitial channels at time $t=0$ when there is no analyte present in the column, mol/m <sup>3</sup>	$r_p$	radius of the charged spherical non-porous particles packed in the column, m
$C_{-\infty}$	concentration of the anions in the electroneutral core region of the interstitial channels at time $t=0$ when there is no analyte present in the column, mol/m <sup>3</sup>	$T$	absolute temperature, K
$D_i$	effective molecular diffusion coefficient of component $i$ ( $i = 1, 2, 3$ ) in the interstitial channels for bulk flow, m <sup>2</sup> /s	$t$	time, s
$E_x$	applied electric potential difference per unit length along the axial direction, $x$ , of the column, J/C/m	$t_{pd}$	duration time of the pulse injection, s
$e$	charge of one electron, C	$v_{elph,i}$	electrophoretic velocity of component $i$ ( $i = 1, 2, 3$ ), m/s
$F$	Faraday constant, C/mol	$\langle v_x \rangle$	electroosmotic velocity in the interstitial channels for bulk flow in the packed bed, m/s
$i_x$	axial component of the current density vector, C/m <sup>2</sup> /s	$x$	axial coordinate of the column, m
$i_x _{t=0}$	axial component of the current density vector at time $t=0$ when only the electrolyte species are present in the column, C/m <sup>2</sup> /s	$z_i$	charge number of component $i$ ( $i = 1, 2, 3$ ), dimensionless
$K_{A,3}$	equilibrium adsorption constant of the positively charged analyte (component 3), dimensionless	<i>Greek letters</i>	
		$\delta$	fixed charge density on the wall of the interstitial channels for bulk flow formed by the surfaces of the packed charged adsorbent particles, C/m <sup>2</sup>
		$\delta_0$	fixed charge density on the wall of the interstitial channels for bulk flow formed by the surfaces of the packed charged adsorbent particles at $t=0$ , C/m <sup>2</sup>
		$\varepsilon$	dielectric constant of the mobile liquid phase, dimensionless
		$\varepsilon_b$	porosity of the packed bed, dimensionless
		$\varepsilon_0$	permittivity of free space, C <sup>2</sup> /(N·m <sup>2</sup> )
		$\gamma_2$	parameter representing the ratio of the electroosmotic velocity of the mobile liquid phase to the electrophoretic velocity of the anion, dimensionless
		$\gamma_{2,max}$	maximum value of $\gamma_2$ , dimensionless
		$\gamma_{2,min}$	minimum value of $\gamma_2$ , dimensionless
		$\lambda$	characteristic thickness of the double layer, m

$\mu$	viscosity of the mobile liquid phase, kg/m/s
$\nu_i$	electrophoretic mobility of component $i$ , $\nu_i = D_i/kN_0T$ ( $i=1, 2, 3$ ), mol·m/N/s
$\rho$	mass density of the mobile liquid phase, kg/m <sup>3</sup>
$\sigma$	conductivity of the mobile liquid phase, C <sup>2</sup> /N·m <sup>2</sup> /s
$\Phi$	electrostatic potential along the radius of the interstitial channels for bulk flow at time $t$ and position $x$ in the column, J/C
$\Phi(r=R_{ic})$	electrostatic potential at the surface of the interstitial channels for bulk flow at time $t$ and position $x$ in the column, J/C
$\chi$	conductivity factor, dimensionless
$\chi_1$	conductivity factor defined after Eq. (8), dimensionless
$\xi$	column phase ratio, m <sup>2</sup> /m <sup>3</sup>
$\Omega_i$	sum of the electroosmotic and electrophoretic velocities of species $i$ ( $\Omega_i = \langle v_x \rangle + \nu_i z_i F E_x = \langle v_x \rangle + (z_i e D_i E_x)/(kT)$ for $i=1, 2, 3$ ), m/s

*Subscripts*

1	cation
2	anion
3	positively charged analyte

**Acknowledgements**

The authors are grateful to Dr N. Leventis of the Department of Chemistry of the University of Missouri-Rolla and Dr J. Ståhlberg of AstraZeneca in Södertälje, Sweden, and of the Department of Analytical Chemistry of Uppsala University in Uppsala, Sweden, for helpful discussions. The authors also gratefully acknowledge support of this work by the University of Missouri Research Board, Criofarma, and the Biochemical Processing Institute of the University of Missouri-Rolla.

**References**

- [1] A.I. Liapis, B.A. Grimes, J. Chromatogr. A 877 (2000) 181.
- [2] B.A. Grimes, A.I. Liapis, J. Colloid Interf. Sci. 234 (2001) 223.
- [3] J. Ståhlberg, Anal. Chem. 69 (1997) 3812.
- [4] S.K. Griffiths, R.H. Nilson, Anal. Chem. 71 (1999) 5522.
- [5] E.B. Cummings, S.K. Griffiths, R.H. Nilson, P.H. Paul, Anal. Chem. 72 (2000) 2526.
- [6] A.I. Liapis, B.A. Grimes, J. Colloid Interf. Sci. 229 (2000) 540.
- [7] B.A. Grimes, J.J. Meyers, A.I. Liapis, J. Chromatogr. A 890 (2000) 61.